



INTERNATIONAL ATOMIC ENERGY AGENCY  
UNITED NATIONS EDUCATIONAL, SCIENTIFIC AND CULTURAL ORGANIZATION  
**INTERNATIONAL CENTRE FOR THEORETICAL PHYSICS**  
I.C.T.P., P.O. BOX 586, 34100 TRIESTE, ITALY, CABLE: CENTRATOM TRIESTE



SMR/754 - 3

**WORKSHOP ON  
SCIENCE AND TECHNOLOGY OF THIN FILMS**

( 7 - 25 March 1994 )

---

" Magnetic Properties and Preparation of Thin-film Magnetic Recording Media "

presented by:

**J.C. LODDER**  
University of Twente  
MESA Research Institute  
P.O. Box 217  
7500 AE Enschede  
The Netherlands

## Chapter 3

### MAGNETIC PROPERTIES AND PREPARATION OF THIN-FILM MAGNETIC RECORDING MEDIA.

J.C.LODDER  
*MESA Research Institute*  
*University of Twente*  
*P.O.Box 217*  
*7500 AE Enschede*  
*The Netherlands*

#### 1. Introduction

Information can be recorded by a variety of methods. In this paper we will concentrate on Magnetic Recording (MR) but where possible Magneto-Optic Recording (MOR) will be mentioned. Both principles can be used in various applications like audio, video or data handling. Furthermore each application has its own type of media in the form of tape, floppy or hard disk. At present the MOR media are only available on hard disks.

In the case of longitudinal and perpendicular magnetic recording the development is concentrated on the following areas of media research:

- Appropriate (higher) coercivities, which means improving the magnetic crystalline anisotropy, the crystal (columnar) size and the microstructure of the boundary.
- Low media noise from the transition even at very short wavelengths, which means a grain (columnar) separation which decreases the inter-columnar magnetic exchange coupling.
- At high density a high output signal, which can be related to the magnitude (chemical composition) and the direction of the magnetisation (the direction of the total anisotropy determined by the shape and crystalline anisotropy).

From a design point of view many improvements can be carried out for realising magnetic recording systems having very high bit recording (several gigabit per square inch). A classical example is the development through the years of the IBM disk system in which big areal-density improvements have been achieved for head, disk and channel technologies [2].

In fig.1 the various dimensions for track pitch, bit-cell length, head gap, medium thickness and head-disk spacing are given as functions of time. It can be clearly seen that all aspects have to be scaled down drastically. The development of (new) thin-film magnetic recording media is one of the possibilities for increasing the recording density. Besides scientific and technical arguments lower costs and higher capacity have also encouraged the magnetic recording industries to research these types of media. Thin-film media are already available commercially in MO-disks, Metal Evaporated Tape (ME-tape) for audio application and Electro(less) deposited hard disks for data recording.

It can be clearly stated that the next generation of magnetic and magneto-optic recording products will all be dependant on the advances in the volume packing density of recorded information.

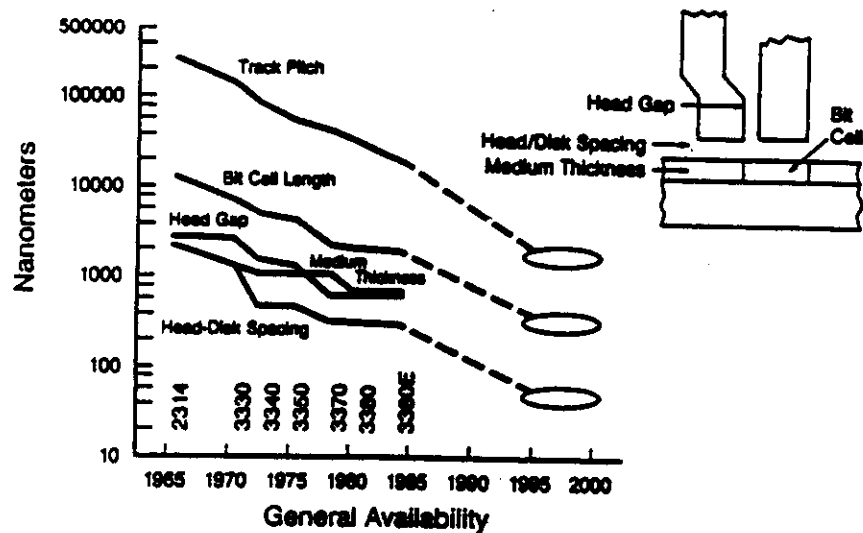


Figure 1. Recording System Scaling [2].

Consequently there is not only a future for thin-film media but also for thin-film magnetic recording heads (smaller gap and track widths) based on inductive reading and writing as well as magnetoresistive reading. As can be seen in the other sections of this book the encoding of information can be done analogously and digitally.

Although the latter has already been successfully applied in data recording there is a trend to use this recording method also for Video (HDTV) and Audio applications (DCC) because errors can be corrected dynamically.

The reconstruction of the original information can be carried out very precisely. It is not essential for understanding and discussing thin-film media to differentiate between digital and analog recording media

Although many different thin-film configurations have been developed for the various fields of application in general, the following essential design parts are given in fig.2.

As can be seen in fig.2 the media consists of a substrate (made of glass, aluminium, polyester, PET etc.), an undercoat (transition-, intermediate- or seed-layer) between the substrate and the magnetic (recording) layer and an overcoat or covering layer. These all consist of different materials and properties, such as chemical compositions, microstructures and thicknesses.

### 1.1 RECORDING MODES

At present we have two modes of magnetic recording dependent on the direction of the magnetisation namely Longitudinal (LMR) and Perpendicular Magnetic Recording (PMR). In the first the magnetic anisotropy lies in the plane of the film and in the case of the PMR media the anisotropy is directed parallel to the film normal. Magneto-Optic Recording (MOR) also requires

a perpendicular magnetic anisotropy. The basic elements of a recording system are given in and consist of a medium with in-plane magnetisation and a ring head.

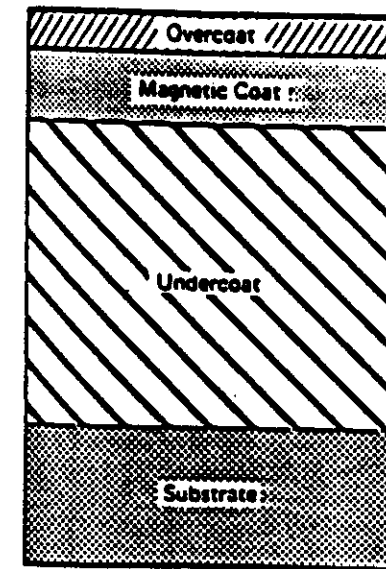


Figure 2. Typical configuration of a thin film media.

The data may be stored in parallel tracks. High density recording depends entirely on how to shorten the recording wavelengths ( $\lambda$ ) and how to narrow the trackwidth ( $w$ )

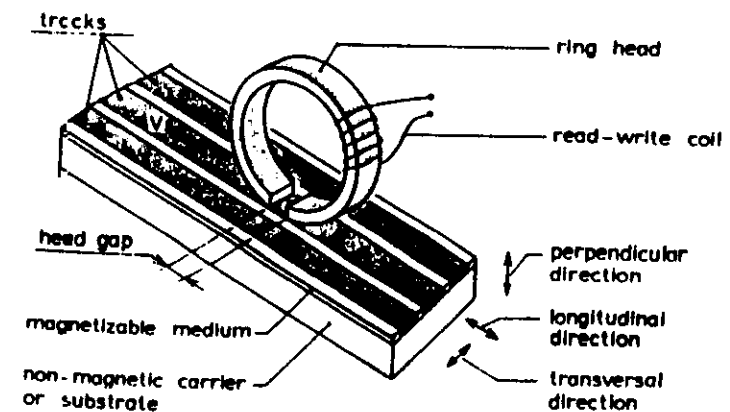


Figure 3. Conventional configuration of a recording system showing the different components and directions [13].

For more information about basic recording principles standard literature is given in the reference list [3-6]. There are two principle techniques for the preparation of magnetic recording media namely 'particulate' coated media and 'thin-film' media. The first one consists of discrete magnetic particles dispersed in organic resins and the second is made by depositing a continuous layer of a magnetic metal, alloy or oxide on the substrate. The magnetic layer thickness for a thin-film media varies from 50-500 nm.

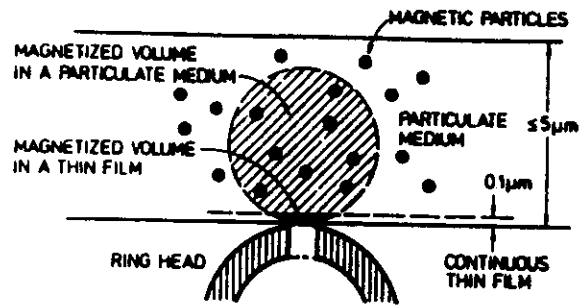


Figure 4. Comparison between the magnetised volumes in particulate and thin-film media.[7]

The general properties for MR media are a sufficient magnetisation ( $M$ ) for reading by the head with an acceptable S/N and an acceptable field strength (which is directly related to the coercivity  $H_c$ ) to create a magnetisation reversal. This field should not be too high for successful writing by the head but it must be large enough to guard the medium against unwelcome reduction of the signal during storage. For high density recording a major potential for changing the signal during the required storage time is the self-demagnetising field originated in the material itself and is proportional to the medium magnetisation. Consequently the  $H_c$  becomes higher for more strongly magnetisable media and that is the case if the recording density increases.

In fig. 4 the interaction between head and medium is given for a (traditional) particle medium ( $\gamma\text{-Fe}_2\text{O}_3$  or  $\text{CrO}_2$  suspended in a plastic matrix) and a thin-film medium [7]. The packing density and the magnetisation of the oxide materials is relatively small [8]. Consequently the magnetised volume must include a large number of particles for a sufficiently high S/N. Figure 4 shows the comparison between the two magnetised volumes of the particle medium and the thin-film medium. The magnetised volume is determined by the condition that the parallel component of the ring-head field is equal to or larger than the  $H_c$  of the medium. This condition leads to a cylindrical magnetised area of which the diameter is proportional to  $1/H_c$  [9]. Depending on the particle dimensions the medium thickness should be in the order of mm's and this limits the minimum recordable  $\lambda$ . Contrary to this, thin-films for media application can be produced with high magnetisations and very thin layer thicknesses. Consequently the magnetised volume decreases and the  $\lambda$  increases.

## 2. Magnetic Properties Of The Media

The media used for recording are termed "magnetically hard" (in comparison with permanent magnet materials it is better to define them as "semi-hard") while magnetic head materials have properties of a "soft" magnetic material. Furthermore the media should have a magnetic

anisotropy in plane (LMR) and perpendicular one (PMR, MOR) to the film surface.

The well-known recording media are made from Fe, Co and Ni alloys and oxides. Their characteristics are described by intrinsic and extrinsic properties (see Table 1).

Intrinsic	Extrinsic
Saturation Magnetisation ( $M_s$ )	Remanent Magnetisation ( $M_r$ )
Crystal anisotropy ( $K$ )	Coercivity ( $H_c$ )
Curie temperature ( $T_c$ )	Permeability ( $\mu$ )
Magnetostriction ( $\lambda$ )	

The intrinsic properties are determined by the type and number of atoms, their arrangement in the structure and their temperature. The extrinsic properties can, in addition, be influenced by the size and shape of the magnetic "units". Therefore in the case of thin-film media the microstructure and morphology play key roles in determining the extrinsic properties. All parameters mentioned in the table are important and have to be optimised for good medium performances.

### 2.1 HYSTERESIS LOOP

In the case of a typical recording medium the hysteresis loop gives the relation between the magnetisation ( $M$ ) and the applied field ( $H$ ).

The value  $H_c$  is the coercivity at a field ( $H$ ) to reduce the component of  $M$ , in the direction of  $H$ , to zero. This is more or less a formal definition. The physical meaning of  $H_c$  is dependent on the magnetisation process involved and may be the nucleation field, the domain-wall coercive field or the anisotropy field.

The intrinsic saturation magnetisation  $M_s$  can be approached at high  $H$  and at zero field the so-called remanent magnetisation ( $M_r$ ) is reached. The loop squareness is defined as  $S=M_r/M_s$ . For the Switching Field distribution (SFD) see paragraph 2.5.

In principle the hysteresis loop of fig.5 shows the behaviour for the easy axis of magnetisation (in the anisotropy direction). This loop has a rectangular shape and exhibits irreversible changes of magnetisation while the hard-axis loop (perpendicular to the easy-axis loop) is more or less linear between the saturation fields and theoretically, hysteresis free.

In general the following is valid for LMR: the higher the value of  $M_s$  the higher will be the value of  $M_r$  and the higher will be the magnetic flux for the reading.

**2.1.1. Coercivity of Thin-Film Media.** The coercivity of a magnetic film is a very complicated parameter and should be discussed in relation to the reversal mechanism and the magnetic microstructure. The morphology of the layer i.e. shape and dimensions of the crystallites (columns), nature of the boundaries, surface and initial layer properties determines how the magnetisation can be reversed by domain-wall motion or by incoherent rotation.

The relation between  $H_c$  and the particle size is given by [10]. The maximum  $H_c$  value is dependent on the thickness for different compositions for longitudinal materials like Co-Ni-(X) alloys [11] as well as perpendicular Co-Cr media [12].

This shows clearly the influence of the microstructure (which develops as a function of the thickness) on the magnetic behaviour.

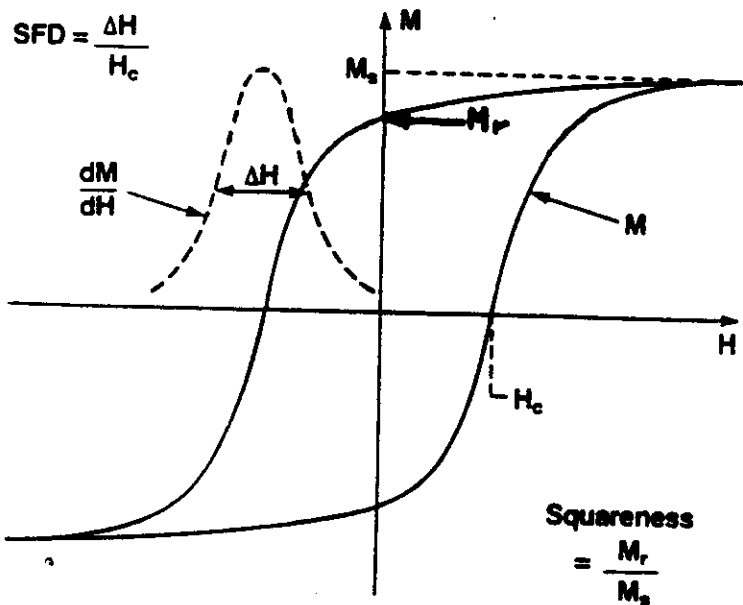


Figure 5. Hysteresis loop of a magnetic recording medium.

2.2. DEMAGNETISING FIELDS.

The shape of a magnetic media (sample geometry) is the most obvious feature which may influence the anisotropy. Depending on the geometry there will be a "charge" at the surface of the uniformly magnetised sheet, cylinder or sphere. This magnetic pole density produces an internal uniform demagnetising field  $H_d (= -N_d M)$  which is, in fact, proportional to  $M$  with an opposite direction.

Here  $N_d$  is the linear demagnetising factor. The sum of the three orthogonal factors is equal to one ( $N = N_x + N_y + N_z = 1$ ). The values for the three factors depend on the shape of the magnetic unit. An important factor is that the magnitude of the internal field ( $H_{int}$ ) is less than that of the applied field ( $H_{app}$ ) by an amount equal to the  $H_d$ . Consequently the  $H_{app}$  must overcome the  $H_d$  in order to saturate the material. It is important for magnetic recording media to realise that the internal microstructure as well as the macroscopical shape can limit the internal magnetising field.

In the case of PMR and MOR the anisotropy must be perpendicular, which means that the highest demagnetisation field is directed opposite to the magnetisation of the sample. This means that the anisotropy energy in the perpendicular direction should be larger than the demagnetising

energy for the perpendicular direction of the magnetisation. In fig.6 the initial states of the magnetisation for the two modes of recording are given. In both cases two written bits with their direction of magnetisation opposite and parallel to the anisotropy direction are drawn. In fig.6a the transitions with uniform magnetisation and zero width can be seen. The corresponding magnetisations and demagnetising fields are shown in fig.6b.

In contrast to the longitudinal mode the  $H_d$  in the perpendicular mode vanishes at the transition.

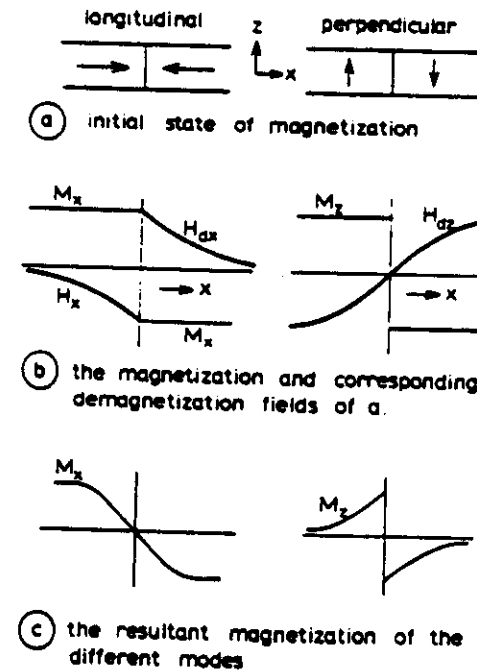


Figure 6. Schematic presentation of the realisation of a transition in LMR and PMR media [13].

Consequently, the longitudinal transition will be spread out, in contrast with the perpendicular transition, which is sharpened (see fig.6c). This principle shows the advantage of the perpendicular mode for very high density transition recording [13].

Another way to consider this point is by comparing the demagnetising factors for longitudinal  $N_l$  and  $N_p$  in the perpendicular direction [14]. If the medium is sinusoidally magnetised with a wave length  $\lambda$ , uniformly through the thickness  $h$  and over an infinite track width, the demagnetising factors are given by:  $N_l = 1 - 1/2 \times h \{1 - \exp(-2\pi h/\lambda)\}$  and  $N_p = 1 - N_l$ . It is simple to show, that  $N_p < N_l$  for  $\lambda/h < 4$ . In fact  $N_p$  approaches zero for infinite bit density.

This schematical presentation (fig.6) shows clearly why demagnetisation is not expected to limit the bit density in perpendicular recording but, on the contrary, will establish a more stable magnetisation at high bit densities than for longitudinal recording.

The recorded bits LMR media are shown in fig.7. For very high densities the written bit is enlarged separately above the figure and from this it can be seen that as the bit length ( $\lambda/2$ )

approaches zero at high densities the  $H_{dx}$  for longitudinal recorded bits approaches one whereas the transition ( $M_x$ ) becomes unsharp (see also fig.6). At very high bit densities, the media must be very thin (10-50 nm), but the perpendicular media can still be between 50-250 nm.

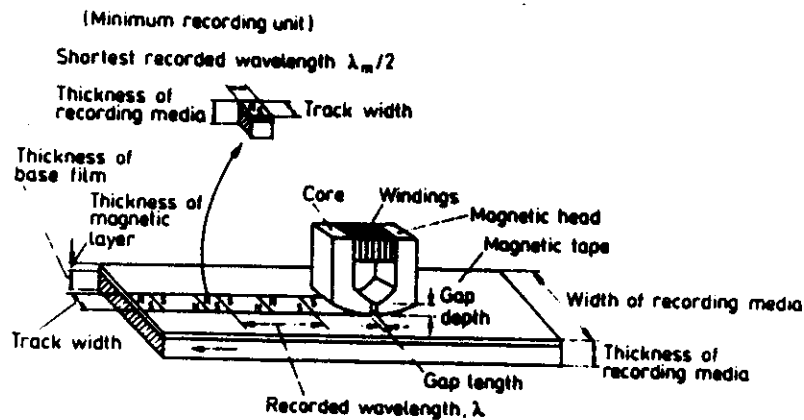


Figure 7. Written bits in LMR media [15].

### 2.3 MAGNETIC ANISOTROPY

Many magnetic samples show preferential directions for the alignment of the magnetisation. These directions are energetically favourable and called easy axes. The energetically unfavourable directions are known as hard axes and are rotated  $90^\circ$  from the easy axes. When a material has only one hard or easy axis the material is said to have uniaxial magnetic anisotropy. (Multiaxial anisotropy occurs in some materials but is less common).

The presence of anisotropy in thin films can be influenced by many different phenomena related to the method of preparation, growth parameters and materials used:

- the incoming energy of the flux atoms during deposition which influence the nucleation and growth process of the film
- the incoming angle of the flux atoms
- the substrate temperature
- preferential growth of the material
- kind of seed layer and the measure of epitaxy
- compositional separation
- impurities
- imperfections of the lattice and/or mismatch between substrate and film

Consequently the formation of uniaxial anisotropy is influenced by many factors, such as crystal symmetry, preferential (poly) crystallite orientation (texture), shape of the sample and stresses.

Some of the major anisotropy forces in recording media are: shape anisotropy, crystal anisotropy, strain anisotropy, exchange anisotropy and surface anisotropy. In the case of multilayers for magneto-optic recording the so-called interface anisotropy (related to the surface

anisotropy and strain) also has a great influence. The strength of the anisotropy determines the difficulty of rotating the magnetisation direction away from its stable alignment with the preferred axis and is thus an influencing factor for the magnitude of the coercivity. The shape anisotropy is caused, as mentioned previously, by the difference between the demagnetising energies in the perpendicular and in-plane directions. This anisotropy is inherently uniaxial. Magneto-crystalline anisotropy arises from exchange forces within the crystal lattice and is, therefore, an intrinsic material parameter in contrast to the shape anisotropy. It is sensitive to temperature and stress and it can undergo irreversible changes if the site occupancy of the ions changes.

Last but not least the strain anisotropy can play a significant role in the total anisotropy. It can be caused by stresses in magnetostrictive materials. The total anisotropy acting in a material is the sum of the three types of anisotropy mentioned. Depending on the character of the thin film (particulate or continuous) and the contributions of the other anisotropies the preferred direction of the magnetisation will be in-plane or perpendicular or somewhere in between.

The most simple way to describe the total anisotropy in a media is to consider the contribution of the different types of anisotropies to the uniaxial anisotropy. First of all we consider the uniaxial magnetocrystalline anisotropy energy density  $E_u$  namely:

$$E_u = K_{u1} \sin^2 \theta + K_{u2} \sin^4 \theta + \dots$$

In this expression  $\theta$  is the angle between  $M$  and the symmetry axis which will be the hard or easy axis depending on whether the uniaxial magnetocrystalline anisotropy constant is positive or negative. In the case of hcp Co the easy axis of the uniaxial magnetocrystalline anisotropy lies parallel to the c-axis of the Co crystal. Usually the first-order term sufficiently describes the anisotropy and we can then describe the anisotropy with  $K_u$  ( $E_u = K_u \sin^2 \theta$ ).

The next contribution to the anisotropy is due to the shape of the material to be considered. For a needle-like particle (z-axis  $>$  x-axis = y-axis) the shape anisotropy can be described by:

$$E_\phi = \frac{1}{2} \mu_0 M_s^2 (N_x - N_z) \sin^2 \theta$$

The corresponding anisotropy field is  $H_m = (N_x - N_z) M_s$ . In the case of a thin film with a thickness very much smaller than the lateral dimensions and thus  $N_z = 1$ , perpendicular to the film surface, the demagnetising energy is given by:

$$E_d = -\frac{1}{2} \mu_0 M_s^2 \sin^2 \theta$$

In this case the demagnetising field is  $H_d = -N_z M_s$  or  $H_d = -M_s$

Furthermore we have to consider the influence of the uniaxial stress  $s$ :

$$E_\sigma = -\frac{3}{2} \lambda_s \cdot s \cdot \sin^2 \theta$$

in which  $\lambda_s$  is the saturation magnetostriction. For this the field is  $H_\sigma = 3 \lambda \sigma / M_s$ , the value can be positive (easy axis coincides with the stress direction) or negative (easy axis  $90^\circ$  from the stress direction) which depends on the signs of  $\lambda$  and  $\sigma$ .

The total uniaxial anisotropy can be given by:

$$E_t = E_u + E_d + E_s$$

If other sources of anisotropy are present we also have to add them to this total contribution. The total anisotropy, as given above, is thus a combination of crystal texture, columnar shape and internal stresses. It is not only a question of magnitude but also the direction of the anisotropies plays an important role in the case of the recording process which is, in fact, the reversal of the magnetic unit (recorded bit).

Tailoring material properties by process parameters and selection of the materials is a great challenge for the scientist involved.

#### 2.4. MAGNETIC STRUCTURE AND REVERSAL MECHANISM

In metallic thin films the micromagnetic behaviour can be different from those of pure particle media, for instance  $\gamma\text{-Fe}_2\text{O}_3$ . An important characteristic of a thin-film medium is its magnetic microstructure, the magnetic unit (intrinsic domain structure or written bit) in the magnetisable layer which has, in principle, two opposite stable directions parallel to the anisotropy axis. The switching of the magnetic units can be achieved by a sufficient high applied field.

The relation between the applied field and the magnetisation for a magnetic recording medium is given by a hysteresis loop, as shown in fig.5. This figure, measured macroscopically by a VSM (Vibrating Sample Magnetometer), only gives information about the average magnetic properties of the thin film which can be characteristic information for recording media. Due to the small bit size of a medium we are much more interested in the local properties in order to understand the recording performance.

At present many possibilities are available for obtaining more knowledge about the so-called micromagnetic (or mesomagnetic) properties of the media. Well known methods for observing the magnetic domains, domain walls, written bits and stray fields are, the Bitter-colloid SEM method [15], MO Kerr observations [16], Lorentz TEM observations [17], Electron Holography [18], EMPA [19], and MFM [20].

The microstructure of the thin-film medium has a great influence on the magnetic behaviour of the film and determines whether the magnetic behaviour of the layer is continuous or particulate. Both qualifications refer to the amount that forces are able to extend throughout the medium. In a continuous medium the exchange forces are hardly disturbed by structural discontinuities such as crystal boundaries and are continuous within the layer. As a consequence the magnetic domain boundaries usually consist of Bloch line walls, which contain exchange and anisotropy forces. The typification "particulate" refers, in the first instance, to the method of preparation, whereby particles, usually single-domain particles, are compound together with non-magnetic materials. In these media, extensively discussed in one of the other sections of this book, only the exchange forces are restricted to the volume of the particles, which means that they only just show magnetostatic interactions. Within this definition, from the magnetic point of view, it is possible that even thin films can be considered as particulate, showing distinct structural ferromagnetic units such as crystals, columns, or clusters of these separated by non-ferromagnetic materials or voids.

A schematic representation of the microstructure in relation to the magnetic structure (track width and transition width) is given in fig.8. The reversal process involved depends strongly on the nature of the crystal boundaries. Such kinds of microstructures can be influenced by the deposition methods and the nucleation and growth processes of the layers.

If the thin film has a continuous microstructure in which there is an exchange between the magnetic units then, in the remanent magnetic state ( $M_r$  in fig.5), the layer will split up into magnetic domains having their direction of magnetisation antiparallel and separated by a domain

wall. The wall is a transition region in which the spins are rotated from the direction in domain A to the opposite direction (domain B). The thickness of such a  $180^\circ$  wall is determined by a minimising process between the various energies and is, of course, dependent on the type of material ( $\text{Co}=8.4 \text{ nm}$ ;  $\text{Fe}=30 \text{ nm}$ ;  $\text{Ni}=72 \text{ nm}$ ).

If the media consist of isolated ferro-magnetic particles, depending on the dimensions of the particle, they may be multi-domain or single-domain. Below a critical size the particle will become super paramagnetic, or in other words, the thermal activation energy  $kT$  will exceed the particle-anisotropy energy barrier. A typical length of such a particle is smaller than  $10 \text{ nm}$  and is strongly dependent on the material and the shape. The reversal of the magnetisation in this type of particle is caused by the thermal motion.

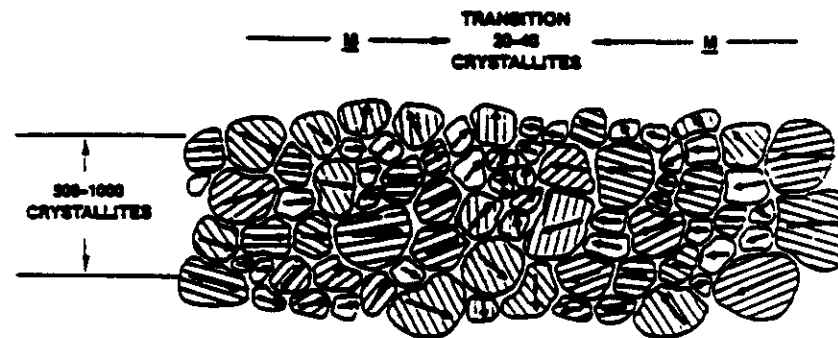


Figure 8. A thin film media track (500-1000 crystals) having an in-plane anisotropy showing a transition width of 20-40 crystals [Hughes 1983].

Single-domain particles (SDP) are defined as particles in which the magnetisation is the same at any point if there is no external field.

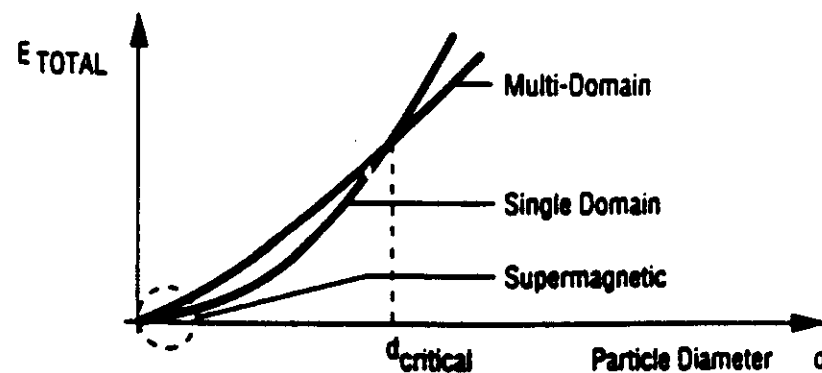


Figure 9. Total energy versus the particle diameter for multi-domain and single-domain particles.

In principle, this is only possible for ellipsoidal shapes but, in practice, if the magnetisation pattern does not differ too much from a homogeneous distribution we still use the term SDP.

In this case the particle will be reversed by a rotation mechanism. The best known reversal mechanisms are coherent (Stoner-Wohlfart particle) and incoherent rotation (fanning, curling, buckling). The other possibility is multi-domain particles (MDP) in which more than one domain can exist. The distribution of domains lowers the magnetostatic energy but increases the exchange energy caused by the domain walls. The reversal in such particles mainly takes place by domain-wall motion.

Fig.9 gives the relation between the total energy and the particle diameter for MDP and SDP. The point where the curves cross a critical diameter is defined as that at which the particle changes from SD to MD. At very low energies super paramagnetic particles can be found. Consequently a decreasing particle size finally reduces the number of domains finally to one.

In fig.10 the relation between the intrinsic coercivity  $H_{ci}$  and the particle diameter ( $D$ ) is given. The maximum is found around the critical particle diameter ( $D_s$ ).

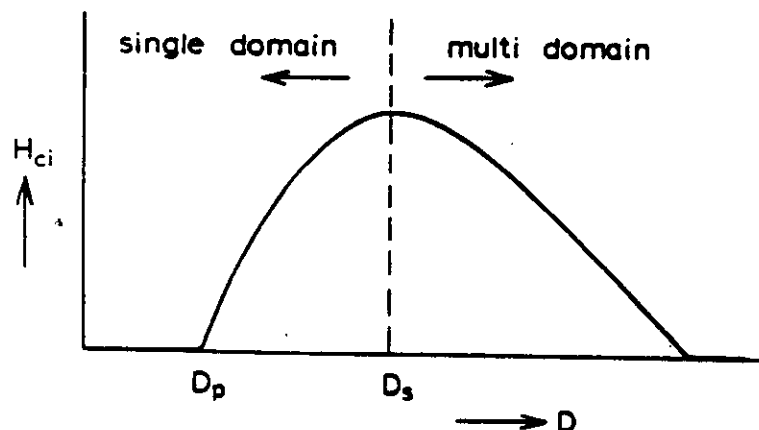


Figure 10. The intrinsic coercivity ( $H_{ci}$ ) of ferromagnetic particles with diameter  $D$ .

Ideal thin-film media should only consist of continuous thin films from the microstructural point of view, but magnetically they should behave as particle media. In other words, for the highest density the crystallites should act as a single-domain particle and magnetically there is no interaction. In this case all the crystallites participate in the recording process with a maximum coercivity. However, in the practical case thin films possess a wide distribution of grain sizes (see fig. 8) and are not completely separated from each other.

In conclusion the magnetisation reversal in thin-film medium is very strongly dependent on the microstructural properties. Depending on the morphology and chemical inhomogeneities of the thin-film media the reversal take place as follows:

- Exchange coupled grains show a magnetic-domain structure which covers many grains and gives a reversal originating from domain-wall motion. The wall energy, influenced by crystalline anisotropy, magnetostatic energy at the wall, strain, chemical inhomogeneities and film-surface properties, dominates the coercivity ( $H_c$ )
- Uncoupled grains which reverse independently. Here the  $H_c$  is determined by the crystalline

anisotropy of the grain, its shape and strain anisotropy.

- Clusters of grains which are locally magnetically coupled can reverse in unison. These reversals are independent of other clusters.

Recently several studies have been published about the relationship of anisotropy, coercivity and magnetic microstructure in Co-Pt-(B)-(O), a rf sputtered high density recording medium [21,22]. In this case the development of the microstructure and morphology was explained as a function of the atomic contribution of the different elements. The large (perpendicular) anisotropy is derived from the strong preferential crystallographic orientation in either the [111] fcc phase or the [002] hcp face. The large perpendicular  $H_c$  originates from the shape anisotropy by means of the gapped columnar morphology.

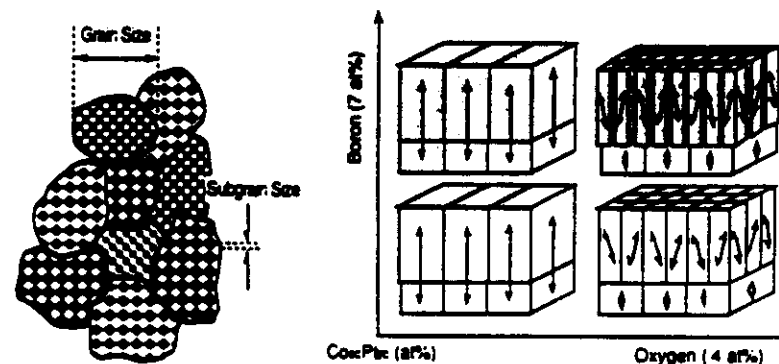


Figure 11. Schematic presentation of the grain structure (left) and the development of the morphology as a function of Boron and Oxygen content in a Co<sub>80</sub>Pt<sub>20</sub> alloy film [22].

Fig.11 schematically represents the grain structure (left) and the development of the columnar morphology of Co-Pt-(B)-(O) films. All films are first deposited on a Pt seed layer 200 nm thickness on a polyimide substrate. The Co-Pt films show a continuous columnar morphology (no gaps). The diameter of the columns is 50-100 nm and the crystallographic structure is identified as fcc. The Co-Pt-O films have indistinct acicular columns of about 10 nm and show a weak [111] orientation. All Co-Pt-B compositions show small sub-grains by adding B of about 2-5 nm while the large grains keep the same value as for Co-Pt. The columnar structure is obscure and the crystallographic directions are more or less randomly distributed. Excessive addition of B changes the structure into an amorphous state in which the fine-grain structure disappears.

## 2.5. SWITCHING FIELD DISTRIBUTION

Another very important macroscopical parameter which can be determined from hysteresis-loop measurements, is the so-called Switching Field Distribution (SFD). In general the fields at which the magnetic units switch are not the same for all of them, but for narrow and stable transitions the SFD should be as low as possible (see fig.5).

The slope of the hysteresis loop at  $H_c$  is also an important parameter. The parameter  $S^*$  can be derived from it.



The so-called Williams and Comstock [23] construction is given in fig.12.. From the slope at  $H_c$  we can write:  $\tan \theta = M_r/H_c = 1 / 1-S^* \Rightarrow dM/dH = M_r/H_c (1-S^*)$

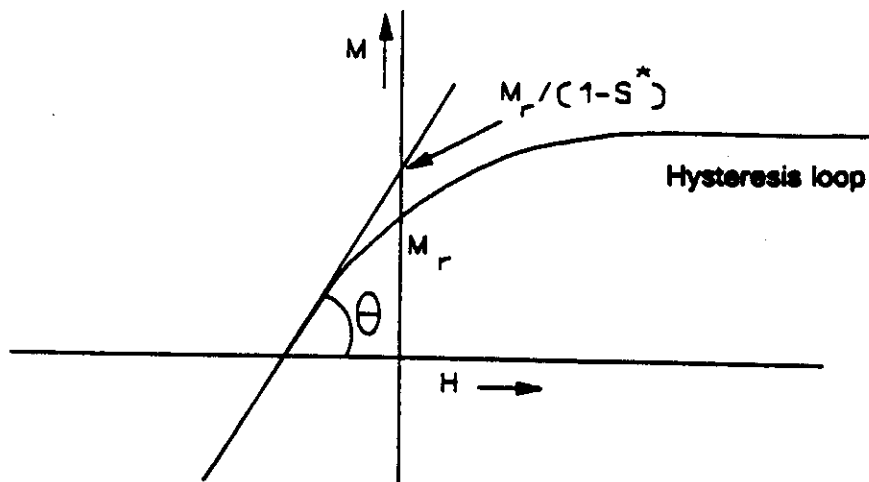


Figure 12. Williams-Comstock construction [23].

It is clear that the  $S^*$  is related to the slope of the loop at  $H_c$ . For longitudinal recording media there are at least two important connections between  $S^*$  and the recording process, namely:

- the maximum output signal is not only dependent on  $M_r$  and  $H_c$  but also on this parameter [24]
- the optimal bias-current is dependent on  $S^*$  [25]

These relations are not valid for media having a perpendicular anisotropy.

Although this parameter is normally used as a SFD parameter, this is not completely correct.. The SFD can be seen as a distribution function of the number of units reversing at a certain field. For a particulate medium without collective behaviour, this function has a close relation to the particle-size distribution, as differently sized and shaped particles reverse at different fields. Of course, the shape and orientation of the particles influence the SFD as well.

In the case of longitudinal media, there are several relations between the SFD and the important recording parameters such as noise, optimal bias current and time-dependent behaviour. Media with a high  $H_c$  and a small SFD are more suitable for high-density recording [26] because the distribution of the switching fields is very small.

An alternative definition is  $SFD = \Delta H/H_c$  (as given in fig.5). In this case the  $\Delta H$  is the full width at half the height of the differentiated loop ( $dM/dH$ ).

It should be clear from this that the magnetic-structure is directly related to the microstructure and chemical inhomogeneities in the layer. The materials used and the deposition process, as well as the parameters also play an important role. Thin-film growth and nucleation processes will therefore be discussed (in relation to the deposition parameters) in the next chapter.

The SFD parameter has been extensively studied for particle media like  $\gamma\text{-Fe}_2\text{O}_3$  and  $\text{CrO}_2$  and also applied recently for perpendicular media [27].

The relations found in the case of in-plane anisotropy are not necessarily valid for media with

perpendicular anisotropy as the demagnetising field has a great influence on the shape of the SFD curve.

### 3. Thin-Film Preparation Technologies

A thin film can be defined as a volume of material deposited on top of a carrier (substrate) with properties differing from it. The interface between the substrate and the thin film has a great influence on the properties of the whole layer. The interface is determined by the properties of the substrate, the material(s) used for a thin film and the method of deposition.

During thin-layer processes the environment can be a liquid, gas or vacuum. Such layers can be deposited by Electro(-less) Deposition (ED), Chemical Vapour Deposition (CVD) and Physical Vapour Deposition (PVD) methods. In the literature various deposition methods are classified in different ways [28-30]. The classification principle used in [28] is based on the concepts of structure and properties of the layers as influenced by the dimensions of the depositing species. There is much to be said about this method because we are interested in the microstructure of the layers due to the fact that it has a great influence on the magnetic properties.

It will be obvious that a close relationship exists between deposition conditions, nucleation and growth of the layer and their physical properties. Thin layers have properties that differ greatly from those of bulk materials. These unique properties can be due to:

- Their small thicknesses; a few atomic layers up to micron values. As a consequence the surface/volume ratio is completely different to that of the bulk.
- Because of their typical growth processes they are found in certain microstructures which are, in many cases, directly related to the physical properties.
- Layer and substrate form a composite system which results in a combination of properties partly based on the substrate properties and partly on the layer itself.
- The interaction between layer and substrate i.e. the interface, mainly defines the structure and properties.

By changing the deposition method and/or varying the different deposition parameters various layer structures and morphologies can be created over a wide range. In contrast to other fabrication methods it is possible to deposit solid materials which can have equilibrium as well as non-equilibrium properties.

In the case of thin-film media for magnetic recording there are in principle four important deposition methods namely: electroless deposition, electrodeposition, vacuum evaporation and sputtering. The first two methods are based on chemical and the other two on physical principles. We first discuss the PVD methods.

#### 3.1. VACUUM EVAPORATION

Evaporation processes are usually carried out under vacuum within a pressure range of  $10^{-5}$  -  $10^{-10}$  Torr. Material vapours are produced by heating the source by direct resistance, radiation, eddy currents, electron beams and laser beam or arc discharges. After evaporation they will condense on a cooler substrate (usually at ground potential).

The low pressure is an essential condition for having as few collisions as possible with background gas species (a straight-line path) and a clean process. During deposition there is a competition between the impinging rate of the rest gases and the nucleated atoms which means the growth of the layer.

The collision rate of gases with surfaces ( $I_g$ ) can be given by:

$$I_g = 3.5 \times 10^{22} P (1/MT)^{1/2} \text{ molecules cm}^{-2} \text{ sec}^{-1}$$

Here  $P$  is the partial pressure,  $M$  the molecular weight and  $T$  the temperature.  $I_g$  is directly proportional to the partial pressure of the particular (rest) gas still available during the deposition.

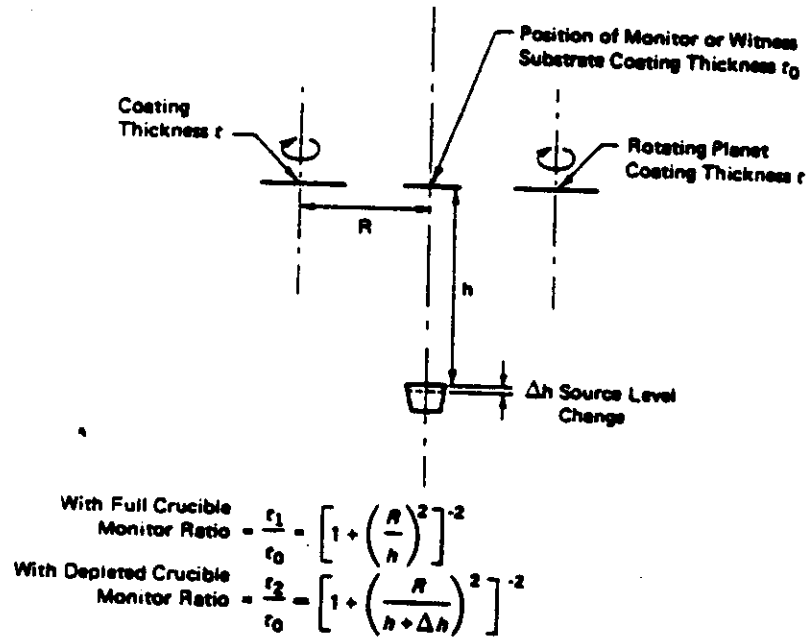


Figure 13. Effect on the coating distribution for full and depleted source [33].

The rest gas is, of course, strongly related to the end pressure and degassing of the system.

The thermodynamical kinetic foundations of the process are given by Glang [31]. In a vacuum the rate of free evaporation is given by the Langmuir-Dushman equation:

$$I_e = 3.5 \times 10^{22} P_e (1/MT)^{1/2} \text{ molecules cm}^{-2} \text{ sec}^{-1}$$

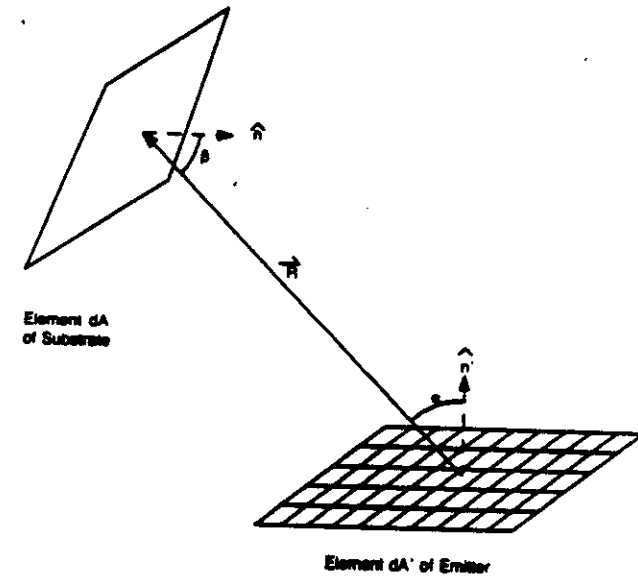
where  $P_e$  is the equilibrium vapour pressure of the source material under saturated vapour conditions with a molecular weight  $M$  and a temperature  $T$ . In non-equilibrium situations  $T_{\text{substrate}} < T_{\text{evaporated matter}}$ . In the first formula, which is the same as the latter for background gas molecules, the source emission geometry, the condensation (sticking) coefficient and the deposition geometry have been neglected. At constant gas and evaporation temperatures the ratio  $I_g/I_e$  is proportional to  $P_g/P_e$ . Low (partial) pressures can be reached using a well-designed pump system and additional methods such a liquid  $N_2$  and outgassing procedures. The emission characteristics (distribution of evaporated molecules) of different types of sources

(point, wire, e-guns etc.) are discussed by Holland [32] in detail.

The growth rate of the deposited layer is unequal to the evaporation rate of the source and depends on:

- the deposition geometry such as the source-to-substrate distance
- the condensation or sticking coefficient which depends on the substrate temperature and surface conditions.

Therefore the coating thickness distribution across the substrate (stationary or moving) is also dependent on these facts. As can be seen in fig.13 even the material level in the source plays a role ( $\Delta h$ ).



$$\text{Number of sputtered atoms/sec on } dA \text{ due to } dA' = \begin{cases} K \left( \frac{\cos \theta \cos \theta' dA}{R^2} \right) dA' & \text{EB, KC} \\ K \left( \frac{\cos \theta dA}{R^2} \right) dA' & \text{SP} \end{cases}$$

Figure 14. Number of deposited atoms for source area element ( $dA'$ ) on the substrate area element ( $dA$ ) for 3 different types of sources [33].

Two practical formulas (see fig.14) can be given for the generalised geometry with  $dA$  (area element of the substrate) and  $dA'$  (of the source) depending on the deposition source, namely electron beam (EB), Knudsen cell (KC) and sputter target (SP).

Unpredictable thickness variations can be expected when deposition takes place with a heated substrate because the sticking coefficient strongly depends on the temperature.

In the case of the deposition of an alloy like the media  $Co-X$  ( $X=Ni, Fe, Cr$ ) the relation between source and film composition should be known. This kind of dependence can be due to a

difference in the evaporation rates because of their different vapour pressures, sticking coefficients and reactions of the individual components with the source. Another problem will be the decomposition of the source if both components are evaporated at different rates. In order to solve these problems a multiple source arrangement can be used (e-guns or others). A wide range of materials can then be evaporated together and form the desired alloys on the substrate. The evaporation rate of each source has to be monitored and controlled separately. By using quartz-crystal layer-thickness monitors the rates can be measured separately during deposition. Various kinds of alloys have been deposited using crystal monitors in combination with an e-gun source [34]. The deposition rate of the components can be measured separately. One rate signal is used to regulate the appropriate rate by controlling the emission current of the e-gun. The other deposition rate is regulated by using the rate signal to control the dwell-time ratio of the electron beam (between the two sources).

The purity and microstructural aspects of films can be influenced by residual gas pressure, evaporation rate, substrate temperature and substrate properties. Some examples of evaporation methods, used for media fabrication, will be described in more detail.

3.1.1. *Reactive Evaporation.* Reactive evaporation is carried out if metal or alloy vapours are produced in combination with a reactive gas.

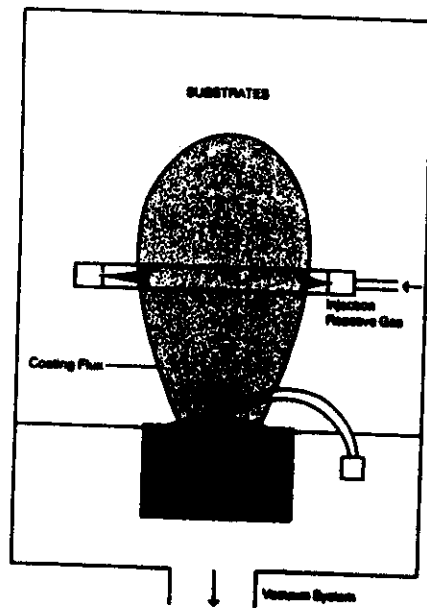


Figure 15. Principle of reactive evaporation with an e-gun.

Consequently a compound will be formed in the gas phase or at the substrate as a result of the reaction between the vapour and gas atoms. The schematic representation is given in fig.15.

In order to produce ferrite films for magnetic applications we have used this method to

produce polycrystalline [35] and epitaxially [36] grown layers. During evaporation a partial  $O_2$  pressure of about  $10^{-4}$  Torr is present. The source material consist of sintered  $MnO$  and  $Fe_2O_3$  powder and was heated by an e-beam. Before  $O_2$  can be admitted the end pressure must be at least  $3 \cdot 10^{-7}$  Torr. During evaporation a partial  $O_2$  pressure of  $10^{-3}$  -  $10^{-4}$  Torr is maintained. Glass substrates are used for preparing polycrystalline layers and  $MgO$  single crystals for epitaxially grown layers. The detailed mechanism of the reactive evaporation process in making  $MnFe_2O_4$  films is not exactly known.

It is also possible to evaporate under a nitrogen gas distribution. Films of Fe-Co-Nitride [37] with very high coercivity and saturation magnetisation have been made. The final structure of these types of films is dependent on the ratio between the metal and the reactive gas particles on the substrate.

The most important parameter for influencing this process is the partial reactive gas pressure and the flow rate. Important parameters are the ratio Fe/Co, the deposition rate and the partial reactive gas pressure and the substrate temperature.

3.1.2. *Vacuum Evaporation of Co-Ni.* Very pure films and to a certain extent preselected structures and morphologies can be obtained by vacuum evaporation. Atoms and molecules are emitted from the source(s) by heating and exist in a gaseous state. The pressure in the vacuum chamber, a certain equilibrium pressure (saturated-vapour pressure  $P_e$ ), is established at a given temperature. The deposition rate ( $R$ ) depends on the vapour pressure. The best results can be obtained if the evaporated elements and their alloys have similar vapour pressures. This is a limitation of the method. In the case of deposition of Co-Ni as a recording media we do not have that problem.

In most cases evaporated films of ferromagnetic materials and their alloys cannot directly attain a suitable coercivity. One of the methods to overcome this problem is to deposit an underlayer between the substrate and the ferromagnetic layer. Lazzari et al. [38] achieved already in 1967 a high coercivity, suitable for magnetic recording, by very slow deposition (0.1 nm/s) of a Co layer (thickness less than 100 nm) onto a Cr underlayer with a bcc structure.

The  $H_c$  was strongly dependent on the rate of deposition, the thickness of the Co as well as the Cr layers and substrate temperature. The Cr underlayer induces growth of the Co layer with an exclusively hexagonal crystalline structure and a very narrow crystallite size distribution. If the Cr layer increases, its crystal size also increases and the Co is grown more quasi-epitaxial. The c-axis orientation of the Co becomes more in-plane if the substrate temperature increases. An important fact is that this effect is stronger if the deposition of Co occurs immediately after the deposition of the Cr underlayer (no oxidation).

Another method to overcome the low  $H_c$  by evaporation is the method of depositing ferromagnetic materials by varying the angle of incidence of the arriving metal atoms [39].

3.1.3. *Vacuum Evaporated Oblique-Incidence Films.* In the early sixties the first paper on NiFe layers evaporated under an angle was published by [40]. The films prepared in this way are very often called "Oblique incidence (OI)" or "Angle of Incidence (AI)" films. It was found that these kinds of films show an anisotropy whose strength depends on the angle of incidence ( $\alpha_i$ ) during deposition. For  $\alpha_i$  between  $0^\circ$  and  $65^\circ$  the anisotropy lies parallel to the film plane and perpendicular to the incidence plane. In [40] the explanation for the anisotropy was based on the self-shadowing mechanism which means that a growing cluster of adatoms causes the shadowing of an adjacent region with respect to the vapour source. Consequently the film grows in chains (columns) oriented perpendicular to the plane of incidence. The shape anisotropy could be the

reason for the macroscopic anisotropy.

Another study [41] was made on the effect of the mobility of metal atoms on the structure of oblique-incidence films and introduced the mechanism of inhibited mobility. The diffusion of the adatoms should be small enough to prevent coverage of the shaded regions. In order to limit this diffusion the substrate temperature should be low, but due to the component of velocity parallel to the substrate of the incoming atoms there is a tendency for them to migrate over the surface into the shaded areas. In order to cope with this the authors introduced the principle of "inhibited mobility" which is based on a position-dependent ratio of residual gas atoms and metal atoms. When this ratio is high the mobility of the adatoms will be strongly reduced due to the increased probability of the formation of bonds (for example oxygen gathering) with the gas atoms. This means that the mobility of the adatoms in the shaded areas is much lower than that of the atoms outside these areas. Trapping of the adatoms in a region with a high oxygen/metal ratio takes place. Applying this principle it is possible to give an explanation for the dependence of the preferred direction of growth on texture, angle of incidence, affinity to oxygen, substrate and source temperature, melting point of the evaporated material and background gas pressure. In another paper from the Philips Laboratory two other authors [42] explain that the shadowing mechanism alone is sufficient to explain the majority features of the microstructure. However in their modelling work they use an atomic relaxation term which shows a strong resemblance to the mechanism of inhibited mobility.

The majority of the publications dealing with oblique-incidence magnetic films have been produced by a group of Japanese researchers [43]. The relation between the columnar inclination angle ( $\beta$ ) and the angle of incidence ( $\alpha$ ) of the evaporation flux was found to be  $2\tan\beta = \tan\alpha$  [44]. The so-called tangent rule is not always valid in a variety of the experimental situations. Besides columnar growth there is another aspect of the morphology namely columnar bundling [45], which is defined as the growth of a column in the direction perpendicular to the evaporation plane. It is also dependant on  $\alpha$ , substrate temperature, rate and gas pressures and even bundling is found in the direction of the evaporation plane.

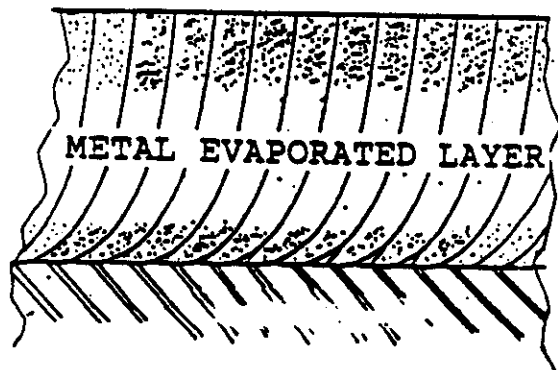


Figure 16. Cross-section of a metal evaporated tape showing the elongated columnar structure.

The interest in OI thin films for magnetic recording purposes is mainly caused by the experimental results that the magnitude and direction of the magnetic anisotropy, the coercivity and a suitable squareness can be varied by  $\alpha$ .

In order to produce the so-called ME (Magnetic Evaporated) tape, modifications relative to the

oblique-incidence evaporation have been made in order to obtain:

- efficient use of the evaporated material
- continuous evaporation over the total length of the substrate, i.e. hundreds of meters of tape have to be produced in one single run at a very high production speed.

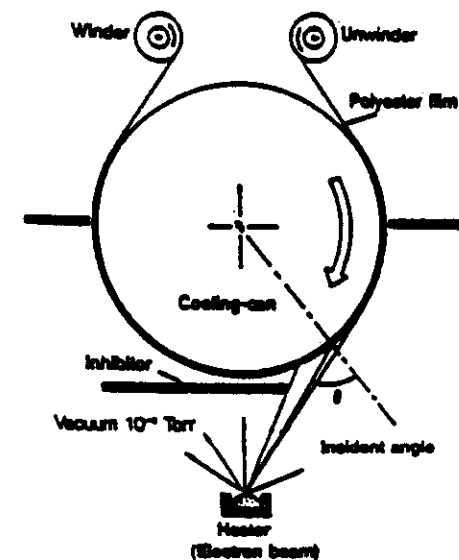


Figure 17. Metal evaporated tape mass-production equipment [46].

The most important modification is that the evaporation occurs over a range of angles, instead of at just one angle, whereby the incidence angle changes as the substrate passes along the vapour beam. This means that the direction of the elongated columns changes throughout the thickness of the tape (see fig.16).

The properties of Continuous Varied Incidence Co, Ni, Co-Ni and Fe tapes were investigated in [46]. A principle deposition geometry is given in fig.17. Depending on the rotation direction of the substrate(tape) two nucleation processes can take place namely:

- High Incidence Nucleation (HIN) in this case the nucleation takes place at high incoming angles of the beam and successive growth occurs with a decreasing incidence angle.
- Low Incidence Angle (LIN) in this case the nucleation starts at low incidence angles and further growth occurs with an increasing incidence angle.

Last but not least the corrosion resistance of this type of material is very poor. Consequently Co-Ni-O results and it is this ternary alloy which has the right magnetic properties. In fig.18 [47] the Hc is plotted versus the Ni wt% in Co for relatively high ( $I = \text{flow } 0.01 \text{ l/min}$ ) and low ( $I = 0 \text{ l/min}$ ) oxygen contents.

The cross-sectional microstructure of a typical ME tape, prepared by ion milling, is shown by a bright-field TEM image in fig.19. Further structural analysis of the tape provides the following data. The thickness of the magnetic layer is about 130 nm and a regular structure composed of very fine fibres is observed (thickness 3-10 nm). The columns make an angle of  $37^\circ$  relative to the plane of the film. AES showed an average composition of  $\text{Co}_{77}\text{Ni}_{10}\text{O}_{13}$  [48,49]. The

substrate side seems to be less dense which is to be expected from large shadowing at a high incidence angle. It is anticipated that the fibre-like structure consists of crystallites. Using X-ray diffraction a hcp Co phase as well as a Ni-O fcc phase is found.

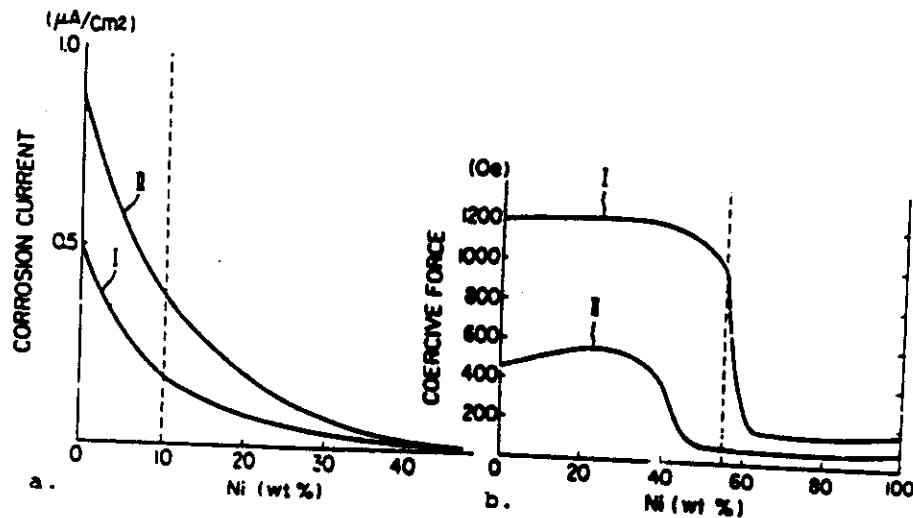


Figure 18. Dependence of the corrosion current and the coercivity on the percentages of Ni and Co for a film with relative high (I) and low (II) oxygen contents [47].

The anisotropy of such a very complicated layer has been analysed [50] while a correlation between the anisotropy direction and the pulse shape has been given in [49].

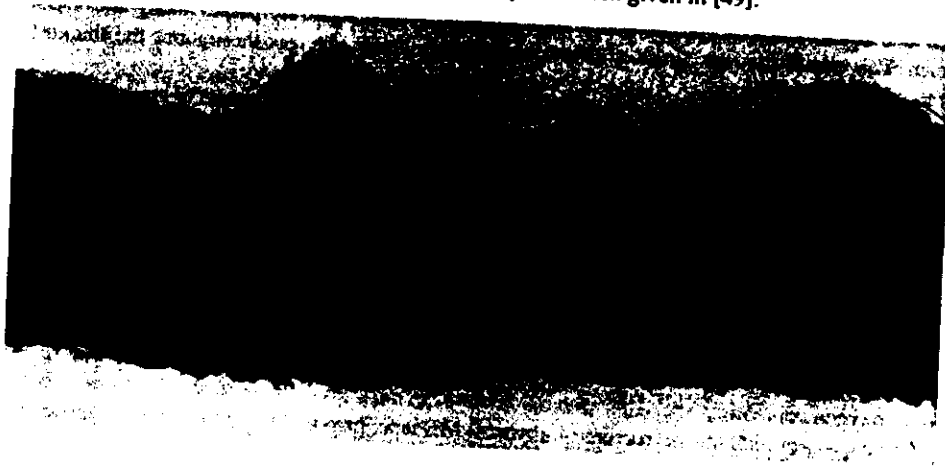


Figure 19. Bright-field TEM image of a cross section of a ME tape.

The angle-of-incidence method has been used for preparation of a hard disk [51].

Two e-gun sources were used and the evaporated beam was deposited at an angle of  $60^\circ$  on both sides of a rotatable disk. The material used was a Fe42.5Co42.5Cr15 layer on a substrate of Al-Mg with an underlayer of stainless steel which needs a special treatment to create the right surface structure of the magnetic layer to prevent adhesive contact between the head and the medium.

Principle studies on the angle of incidence effects were carried out by groups at CNRS Meudon [52] and Twente [53].

### 3.2. GLOW DISCHARGE SPUTTERING

From the physical point of view sputtering is a totally different process to evaporation. Generally, the sputter deposition process concerns the ejection of atoms from the target by energetic particles. The ejected atoms then condense on the substrate to form a thin film. The accepted theory of sputtering is based on Wehner's research [54] which showed that it is a momentum-transfer process.

In the case of systems discussed here, the sputtered atoms leave the target at an appreciable kinetic energy (3-10 eV). Part of this energy will be dissipated by the collision process with atoms of the sputtering gas. Upon arrival at the substrate the energy is still 1-2 eV (evaporation 0.03 eV). Typical deposition rates are 5-50 nm/min.

There are two principle sputtering methods namely:

- Glow-discharge sputtering; a plasma is formed between the target and substrate. The positive gas ions interact with the target material.
- Ion-beam sputtering; here the ion beam is produced in a separate ion gun and directed onto a target.

Because the glow-discharge method is the most important for thin-film media production only this method will be discussed. A glow discharge is formed in a low-pressure gas when a DC voltage is applied across two planar electrodes (cathode - and anode +) at the so-called breakdown voltage [55]. The glow discharge for sputtering is sustained by the secondary electrons which the ions produce on striking the cathode. Each secondary electron produces 10 to 20 ions to sustain the discharge. The principle DC planar diode-sputtering system is shown in fig. 20. The luminous regions of a DC discharge show a dark space near the cathode (target) and the anode (substrate holder). For uniform sputtering of the cathode, the anode should be located at a distance from the cathode of about 2-4 times the thickness of the cathode dark space. This distance is inversely related to the gas pressure. If the pressure is increased to make the dark space small, the deposition rate is limited because the sputtered atoms experience multiple collisions before reaching the substrate plate. (The mean free-path length is a function of the pressure). For DC-sputtering, a practical compromise of  $10^{-2}$  to 0.2 Torr is used for a target substrate distance of 2-5 cm.

In addition to the removal of neutral atoms from the surface of the target by the bombardment of the ionised sputtering gas to form the deposited film, there are several other effects that occur at the target surface which influence the film growth. In fig. 21 the particle mechanism at the target and substrate during sputtering is shown.

With a view to the process of nucleation and growth of the layer, the interaction of particles with the substrate is very important. As can be seen in fig.21 most of these particles are generated

after interaction with the target. The effects of the particles are very complicated, for example the secondary electrons produced at the target surface not only generate secondary positive ions but also a heat flux to the substrate.

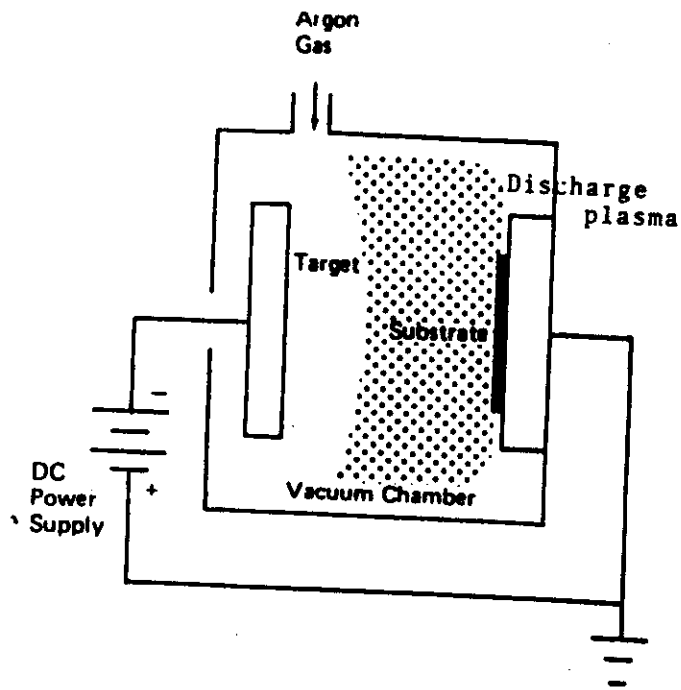


Figure 20 Principle of DC-planar diode sputtering system.

The negative ions of the target material can sputter the already deposited film itself. The characteristics of the film deposited on the substrate will therefore depend on the relative numbers and energies of the various species as they reach the growth surface and their subsequent behaviour. This will depend on a number of factors such as substrate temperature, substrate potential etc. Vossen [24] has mentioned 14 effects which may result from changes in deposition rate, substrate temperature and bombardment of the film by species in the discharge [56]. The effect which different parameters have on the growth of a film may also vary greatly from material to material. A very important characteristic of the sputtering process is the sputter yield; defined as the number of ejected species per incident ion. This parameter increases with the energy and mass of the bombarding ions as well as with increasing obliqueness of the incident ions. In order to obtain the yield for low bombardment energies the following equation can be used [57]:

$$S = 3\alpha / 4\pi^2 \times 4 m_t m_i / (m_i + m_t) \times E / U_0 \quad (\text{atom/ion})$$

where  $\alpha$  is a monotonically increasing function of  $m_t/m_i$  which has values of 0.17 for  $m_t/m_i = 0.1$ ,

increasing up to 1.4 for  $m_t/m_i = 10$ . The values  $m_t$  and  $m_i$  are the masses of the colliding atoms,  $E$  is the energy of the incoming ion and  $U_0$  the surface binding energy. For energies of about 1 KeV a modified equation is given by Chapman [55]. Sputtering yields as a function of the energy for all sorts of materials can be found in the standard literature.

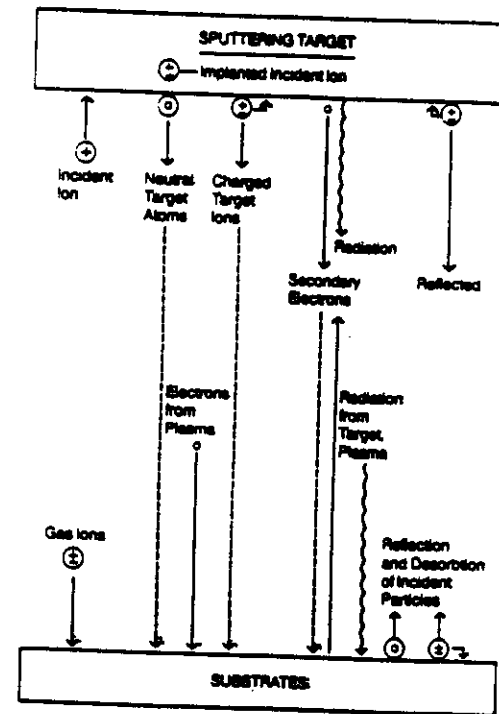


Figure 21. Particle interaction, at the substrate and the target in a glow-discharge sputtering system.

Another sputter parameter which can be used is the choice of the sputter gas. Mostly Ar is used but other gasses for instance Kr and Xe can also be applied as an alternative or in combination with Ar. For instance reflected Kr atoms have less energy than Ar atoms. This can drastically influence the nucleation and growth processes.

The DC configuration cannot be used for sputtering dielectric materials. An RF frequency of 13.56 MHz is used and the generator is coupled through a so-called blocking capacitor to the insulator (target). The target area is small in comparison to the substrate area (the substrate is connected to the system ground and consequently connected to the base plate and walls of the system). The dependence of the ratio of the voltages on the low electrons ( $T$  = target,  $S$  = substrate) and the relative electrode areas is given by [55]:

$$V_T/V_S = [A_S/A_T]^4$$

The exponent can be less than 4.

Between the glow discharge and the electrode is a narrow region in which a change from the plasma potential to the electrode potential occurs. This is called a sheath or dark space. A typical RF diode-sputtering system looks the same as the DC unit.

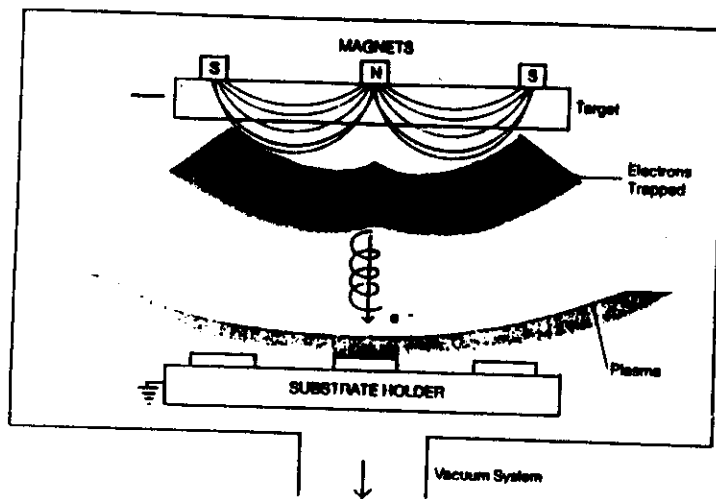


Figure 22. Planar-magnetron sputter system.

The capacitor allows a net negative DC voltage to be developed at the target. The thickness of the dark space and the flow regions are similar to those of the DC mode and are dependent on the gas pressure. In RF sputtering the operating pressure ranges from  $2 \cdot 10^{-3}$  -  $20 \cdot 10^{-3}$  Torr and the commonly used electrode separation is 5 cm. It is, of course, also possible to sputter metals with the RF mode.

**3.2.1. Magnetron Sputtering.** Magnetron sputtering (with DC or RF power) is used to increase ionising efficiency. In normal glow-discharge processes only a few percent of the sputter gas atoms are ionised. A magnetic field normal to the electric field is used to increase the path length of the ionising electrons. There are several configurations, of which the principle one is given in fig. 22 for planar magnetron sputtering.

One of the advantages of magnetron sputtering is that most of the secondary electrons are concentrated directly under the target and do not interact with the substrate resulting in a low substrate temperature (the secondary electrons are responsible for 80 % of the heat flux to the substrate). A further advantage, certainly in the case of production units, is the higher deposition rate and the more efficient use of the target material by an optimal arrangement of the magnets.

**3.2.2. Bias Sputtering** An interesting parameter which depends on the system geometry, sputter conditions, target material and the residual gas pressure is the bias voltage. During sputtering a negative voltage ( $< 200$  eV) is maintained at the substrate holder and this will influence the layer properties by changing the flux and energy of incident (charged) particles. In contrast to normal sputtering, in the case of a bias, some of the positive Ar ions will also reach the substrate surface. Consequently a weak (low-voltage) sputtering effect occurs during film growth. In the case of

small bias voltages the cathode sheath is so thin that this area will be collision free. The following phenomena are present at a biased substrate:

- removal of contamination of the substrate surfaces (sputter-cleaning)
- influencing the growing layer by removing loosely bonded particles and consequently modifying the structure.

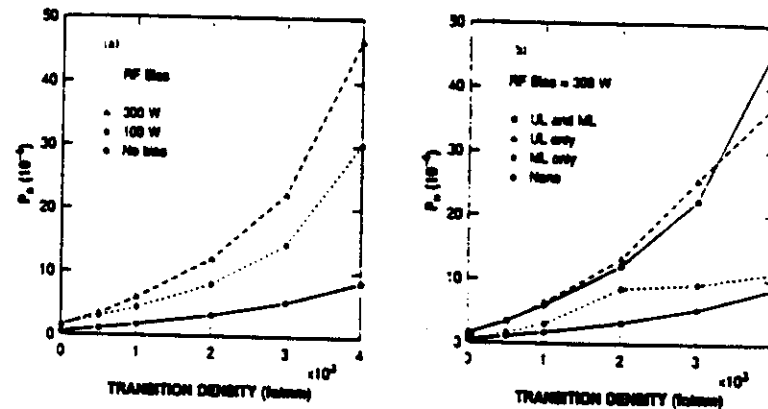


Figure 23. Normalised media-noise power as a function of written transition density, a) when bias is applied to the underlayer and magnetic layer b) when bias power is independently applied to the underlayer and the magnetic layer [64].

For instance the bias voltage can influence the composition of the growing film which is sputtered from an alloyed target [e.g.58], the structural properties [59,60] like crystal size, morphology and related properties such as stress [60], resistivity [61], hardness [62] and dielectric properties [63]. All these properties influence directly or indirectly the final recording performance of the layer.

It was reported [64] that the layer growth morphology of Co-Pt-Cr longitudinal media deposited on a Cr underlayer was influenced by  $V_{bias}$  and therefore has a great influence on the media-noise performance.

In fig.23a the normalised media-noise power is given as a function of written transition density when the rf bias voltage was applied to both layers. With increasing bias it was found from measurements that the surface becomes smoother and the  $H_c$  squareness increases. The media noise increases substantially. The authors also found that by independent biasing the magnetic and non-magnetic underlayer they could influence the growth and consequently the media noise. Biasing only the underlayer the surface of the Cr becomes very smooth and the non-biased magnetic-layer grows like a continuous film which leads to a significant increases of the medium noise. The various possibilities of applying a 300 W bias power are given in fig.23b.

**3.2.3. Reactive Sputtering.** This mode is used to grow compounds or alloys by using a reactive gas environment such as reactive evaporation. The target will be a metal (alloy) or a compound. Many different layers such as oxides, nitrides, sulphides, fluorides etc. have been deposited [65]. The mechanism of reactive sputtering can be generally explained by a chemical reaction at both electrodes (substrate and target). Using a pure metal target the sputter rate then decreases from the metal value to the compound value as the partial pressure of the reactive gas increases because this gas will be adsorbed on the target. This depends on the reactivity between the gas and target

materials. This method was used for perpendicular recording media to prepare thin films consisting of very small ferromagnetic particles. As an example Fe-Co-O films have been prepared in this way [e.g.66]. The relatively large perpendicular anisotropy is due to the strong shape anisotropy of the magnetic metal phase (Fe-Co cubic bcc) in the non-ferromagnetic Fe-oxide phase (Fe-O NaCl-structure). The very small metal fibres (10 nm diameter) grow perpendicular to the substrate surface. In the oxidised state the surface properties are mechanically very stable and suitable for recording.

### 3.3. GROWTH AND MICROSTRUCTURE OF THIN FILMS.

The nucleation and growth processes of a thin film are dependent on the method of deposition and the process parameters used. On the other hand the type of substrate, the use of underlayers (seed layers) and the type of magnetic material also play a very important role. Recently, various papers about magnetic and magneto-optic materials have been published during an MRS symposium held in 1991 [67]. Special attention has been paid to the correlation of the microstructure with the recording performance. In particular the magnetic coupling between grains and/or columns has been discussed in relation with deposition parameters.

**3.3.1. Nucleation and Growth processes.** Using PVD processes the depositing flux will have energies ranging from thermal (0.3 eV) for evaporation and a few eV during sputtering. These energies have an important effect on the processes of nucleation and growth and consequently on the interface formation. If we assume that there is no chemical reaction between the growing layer and the substrate and both are insoluble, the interface which is formed is of the type with an abrupt discontinuity in composition. For instance, this interface can be modified by the application of ions during formation. The layer properties will then be influenced by changing the interface. After an interaction of the vapour stream with the substrate an adatom can be formed if the kinetic energy of the "atom" is small. An adatom is a physically absorbed atom with the probability of becoming desorbed. Adsorption occurs if the binding energy between the atom and surface is large. If the binding energy is small, nucleation, since it is also dependent on the temperature and the vibrational energy at the surface never occurs. Formation of critical nuclei is essential for thin-film growth. A critical nucleus is determined by the interfacial free energy and the free energy per unit volume of the growing nuclei. During the growth of the nuclei two energies are in competition which each other, namely the surface free energy, which increases as the surface area increases and another energy which is the difference between the free energy of the solid and vapour phases.

The thin-film formation process is schematically given in fig. 24 and can be classified by the following stages:

- condensation of an atom (adatoms) and forming nuclei by the migration process (fig. 24-1).
- further growth of critical nuclei which leads to clustering and island forming. Islands grow in size rather than in number (fig. 24-2 / m 4).
- coalescence stage arising from large touching islands (fig. 24-5).
- preceding the coalescence process the film reaches continuity (fig. 24-6).

The nucleation theory (forming nuclei from adatoms) can be explained by two theoretical models [e.g. 68], based on condensation of the vapour phase, namely the atomistic model (few atoms) and the capillary or droplet model (valid from approx. 100 atoms). For the sake of simplicity we can make the assumption that the first model is based on the physical (thermodynamic) theory and the second on chemical principles. With the capillary model the size

of the nuclei (clusters) vary continuously as a function of the free Gibbs' energy while the atomistic model is based on a discontinuous variation of the size as a function of the dissociation energy.

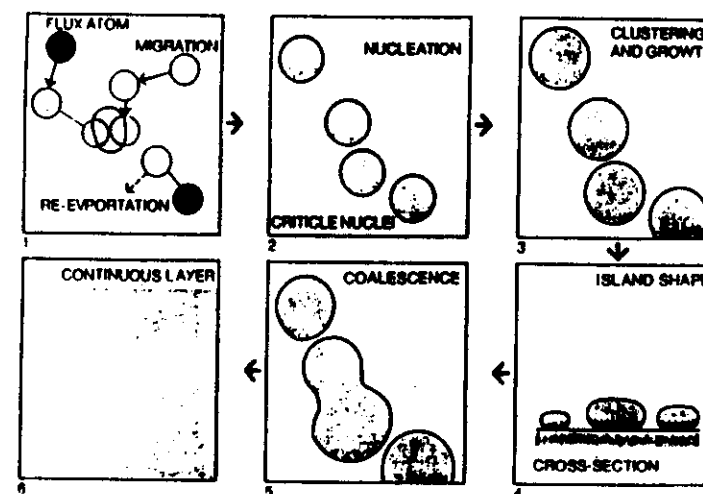


Figure 24. A schematic presentation of the nucleation and growth process of PVD layers.

**3.3.2. Microstructure and morphology.** The process parameters (flux rate, substrate temperature etc.), type of material (desorption, dissociation and diffusion energy terms) and the substrate properties influence the growth process.

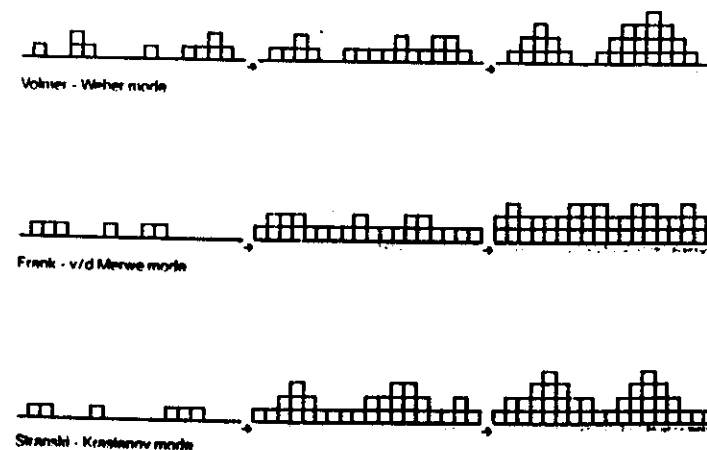


Figure 25. The three basic nucleation models.

Three basic nucleation growth models are known (see fig. 25) namely:



- island or Volmer-Weber mode [69]
- layer or Frank and v.d. Merwe mode [70]
- layer followed by island or Stranski and Krastanov mode [71]

The two latter modes have always been discussed in relation with the growth of single crystals on monocrystalline substrates while the former may occur for either epitaxial or polycrystalline growth. The theoretical basis of having one mode in preference to one of the others (or variations thereof) is principally based on surface-energy considerations. The last two models are always associated with growing single-crystal films on monocrystalline substrates and the Volmer-Weber mode can be used for polycrystalline as well as epitaxially growth.

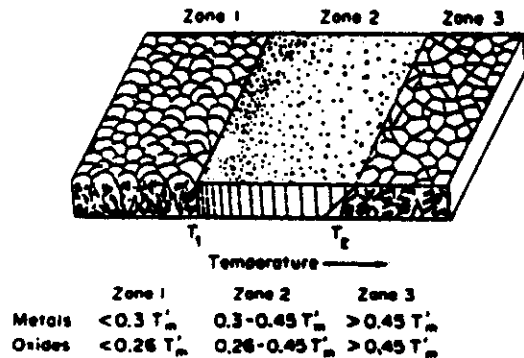


Figure 26. Microstructural model for vacuum-evaporation technology [72].

Depending on the process, film materials and substrate behaviour all types of layer structures can be grown (amorphous, polycrystalline and single crystal). Higher mobility of adatoms makes it possible to create films with deviating stoichiometry. Variations in substrate temperatures even make it possible to deposit metastable structures. With treatment of the substrate surface or deposition of pre-nucleation centres it is also possible to grow films with a preferential crystallographic orientation (texture) and a specific morphology.

The thin-film microstructure can be modified by means of substrate temperature, surface diffusion of the atoms on bombardment during film formation, incorporation of impurity atoms and the angle-of-incidence effect of the incoming particle flux.

In most case the final properties of the deposited layers differ from materials made by standard metallurgical methods. The substrate temperature is the most important process parameter for explaining the morphology of evaporated films [72]. Three different structures are given (see fig. 26) as a function of the ratio substrate temperature ( $T$ )/melting temperature( $T_m$ ). This model is modified for the sputtering process [73] and is extended with a second parameter, namely the Argon pressure. In this model the influence of the surface roughness is also considerable. The principle of the so-called Thomson model for sputtered films is given in fig. 27. This zone-structure model has been revised by Messier [74] and accounts for the evolutionary growth stages of structure developments as well as the separate effects of thermally-and bombardment-induced mobility. In fact it was pointed out by Messier that the pressure axis should in fact be the energy axis. In this case increasing pressure means a decrease of kinetic energy of the sputtered atoms. It is clear from this that application of a bias voltage will influence the energy-axis as well.

Within a certain layer thickness and a special set of process parameters the grain size of the

deposited layer increases with the layer thickness. Usually deposited thin films have a higher defect density than bulk material. The defects in polycrystalline thin films are grain boundaries, column boundaries, voids, vacancies, dislocations and interior gas bubbles.

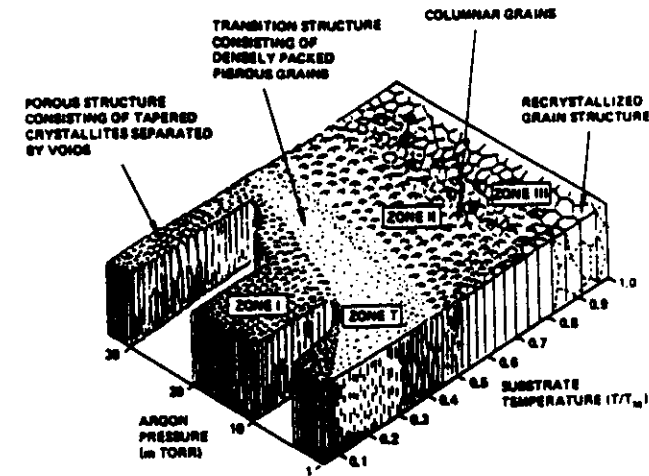


Figure 27. Microstructural model for sputter deposition [73].

Defects are mostly responsible for the low temperature interdiffusion processes. In the case of polycrystalline films the grain boundary is the most important property. Epitaxial growth is a very special form of nucleation as well as growth and has an unique orientation relation with the substrate. Single-crystalline films can be prepared by the correct choice of the substrate material and deposition parameters.

3.3.3. *Computer simulations of the growth.* In order to investigate the nucleation and growth of thin films various computer simulation studies have been made for evaporation as well as for sputtering. We have developed a two-dimensional Monte-Carlo model for thin-film growth in the case of oblique evaporation for one- as well as for two-source deposition [75]. The incoming particles are considered to be spheres. The simulations are related to zones 1 and 2 in fig.26. In the case of zone 1 the incoming atoms have a very limited mobility. Modelling in this way can be very useful for understanding the morphology development of a thin-film layer.

### 3.4. MULTILAYER TECHNOLOGIES.

During the last 20 years enormous advances in thin film preparation processing have been made in the field of so-called artificial structuring of materials; semiconductors, metals and isolators have been prepared in various sizes and geometries. Using metal compounds several classes of layered structures have been made.

In fig.28 a schematic presentations of the multilayer structure (a and b) and some different possibilities for stacking the individual thin layers.(c-f) are given. The total multilayer thickness (fig.28-a) will vary depending on the application but can even be in the micron range while the individual layers (fig.28-b) can be varied from 0.2 to about 5 nm. In the current literature various

names are used for multilayered structures like layered composites, periodically modulated structures, superlattices etc. It is well known that "superlattice" means a regularity in a (single) crystal with a longer wavelength than the unit cell.

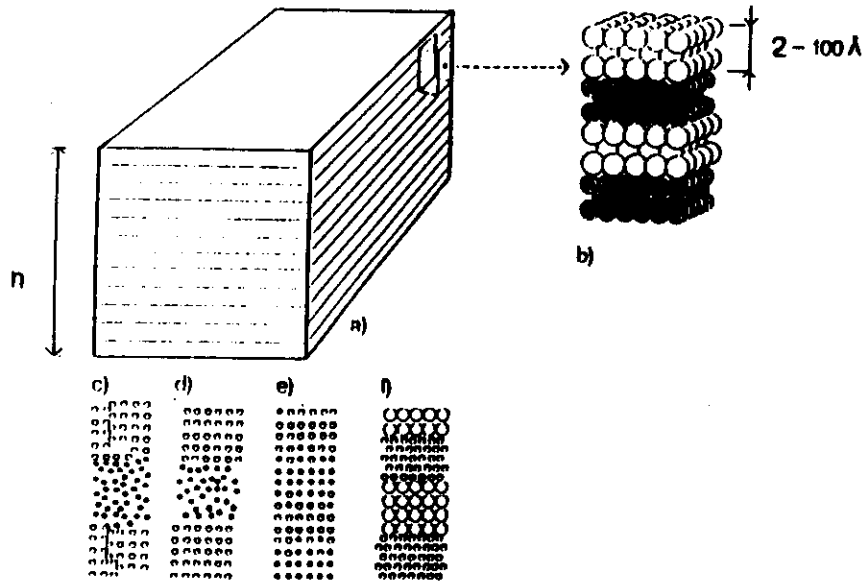


Figure 28. Multilayer structures (a and b) and some different possibilities for stacking the individual thin layers (c-f).

This term has often been used for artificially structured multilayers i.e. a new class of superlattices. The term superlattice is used for all types of packed multilayers whether epitaxial or not [76].

Layered structures can be deposited by sequential deposition of two or more materials. In principle two possibilities are available:

- a sequence control using a shutter.
- rotating the substrate positions with different direct lines from source materials.

An example of a deposition method for preparing multilayers can be seen in fig. 29.

In contrast to the MBE (Molecular Beam Epitaxy) method (UHV pressure range) dual sputtering is also used and the work pressure here is high, namely  $10^{-2}$  -  $10^{-3}$  Torr. This can present problems during stacking of the multilayers on the one hand, but the method is closer to a commercially usable process. With ion-based technologies it is also possible to deposit multilayered structures.

By using ions during layer growth it is also possible to vary the kinetic energy of the beams and alter the growth conditions. After preparing a multilayered (metal) film, by alternating deposition of two elements, a periodicity alloy along the film normal should appear if the following conditions are satisfied:

- the layer thicknesses are on an atomic scale.
- a layered structure is formed.

- the interdiffusion is sufficiently suppressed.

The choice of materials for metallic systems is still expanding and at present various examples of combinations with different atomic radii have been prepared. Here multilayered techniques also show possibilities for new material syntheses. In contrast to materials prepared by chemical procedures superlattices are made far from equilibrium. The various possibilities for layering artificial superlattice materials are given in fig. 28 (c-f). Most of the stacked layers (c,d,f) have more or less sharply defined boundaries and some have a non-crystalline structure in the individual layers (c) or one of the layers is non-crystalline (d). In such situations the structural information is not transmitted between adjacent layers and therefore, strictly speaking, no superlattice is formed. In the case of an unsharp boundary (e), compositionally modulated alloy-layered structures have been made.

The amplitude of composition modulation in the centre of a layer can be in the range of 0 to 100 %. Superlattices can also be formed with sharp boundaries (< 5% of the thinnest layer) between the two components. All these possible combinations strongly affect the electronic and physical properties of materials. Especially when the dimensions of the layer structure become comparable with the characteristic lengths relevant to the properties in the selected materials.

The application of multilayer structures in recording technologies plays an important role. Nowadays multilayer configurations are used in Thin-Film Heads (high Ms and m and also for magnetoresistance type) for magnetic recording as well as in media for Magneto-Optic recording.

Crucial aspects which are important for these types of layers are the sharpness of the interface and the flatness. These aspects are strongly related to the method of preparation, the type of materials and the substrates used. Generally speaking the layer growth mechanism plays the key role in the final interface structures.

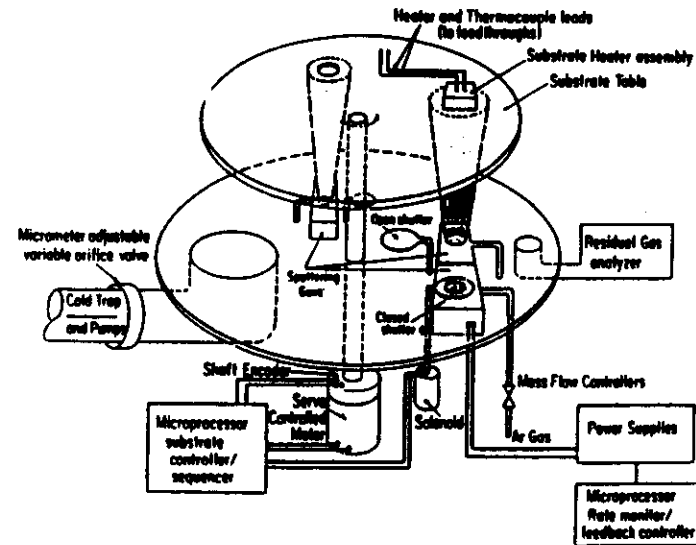


Figure 29. E-beam evaporation for preparing multilayer structures with shutter control.

Later Mn-Al-Ge and Co-Pt were intensively studied followed by Gd-Co but the latter was used for compensation point writing.

However none of these materials was ideal. For instance MnBi consists of two crystallographic phases and is very unstable above 400 °C. The noise problem was high in the case of MnAlGe media and domain instability played the most important role in the case of Gd-Co.

The magneto-optic materials of today have been selected on the basis that they can sustain sub-micron domains, have a large signal-to-noise ratio supported by sufficient magneto-optic effect, resistance to corrosion and are chemically stable. The most popular materials at present are the amorphous rare-earth metals (Gd, Tb and Dy) and transition-metals (Fe, Co) alloys which are deposited by evaporation or sputtering. Alloys like Gd-Tb-Fe and Tb-Fe-Co are well known at present and can be made commercially.

There is also a great interest and a lot of research on so-called multilayer structures for MO application [77]. Mainly Co/Pt and Co/Pd have been studied by evaporation and sputtering. Although both preparation methods shown different physical processes the MO-properties of the films are not very different from each other.

As an example a few aspects of Co-Pd sputtered multilayers are given [78]. The layers have been sputtered at a background pressure of  $1 \cdot 10^{-7}$  Torr. The Si-substrates were positioned below the targets on a rotating table. The Co thickness was between 0.2-2.5 nm and Pd layers of 1.4 nm. Different Ar pressures were used. The number of bilayers (N) was 25 for all films. Most of the films were deposited on a Pd seed layer of 20 nm, and Kr was also used as a sputter-gas. The effective anisotropy (per Co volume) was calculated from torque measurements and also included also the shape anisotropy. In fig. 30 the anisotropy ( $K_{eff} \cdot t_{Co}$ ) versus the layer thickness of Co ( $t_{Co}$ ) is plotted for different gasses, pressures, seed layers and rates.

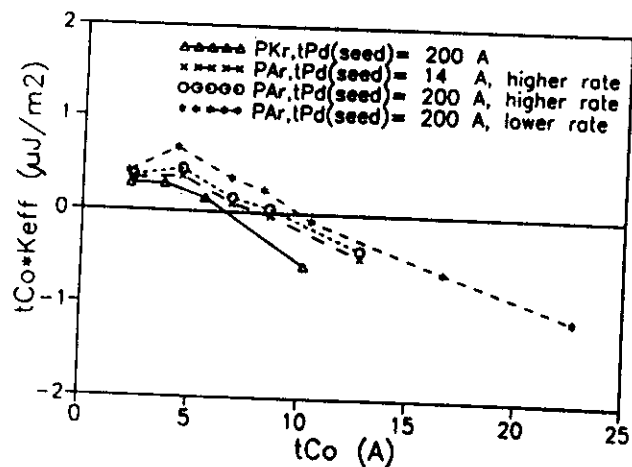


Figure 30. Anisotropy vs. Co layer thicknesses for Co/Pd multilayers sputtered with different deposition parameters [78].

In the literature the following relation is used for interpretation of the various anisotropy contributions  $t_{Co} \cdot K_{eff} = 2 \cdot K_s + t_{Co} \cdot K_v$ ; in which  $K_s$  is the surface anisotropy and  $K_v$  the volume

anisotropy. It would seem from fig.30 that the  $K_v$  for all films sputtered with Ar is the same and independent of the sputter rate and seed layer thickness, which means that the change in the  $K_{eff}$  is due to the change in the  $K_s$ .

### 3.5. ELECTROLESS DEPOSITION PROCESS.

In comparison with the PVD processes the chemical processes (electroless and electro deposition) have a much higher deposition rate and can be sometimes more economical. Electroless (chemical) plating is mostly used for preparing longitudinal and perpendicular media on hard disks. Most of the published work is concentrated on Ni, Co and NiCo alloys obtained from hypophosphite electrolytes. In a standard paper [79] Busic et al. demonstrated that Ni cations could be reduced by  $H_2PO_2^-$  anions to form a Ni deposit containing phosphorous. A similar process is valid for Co deposits. Typical electrolytes for electroless deposition are:

- a salt of the metal ion to be plated
- hypophosphite in the form of the sodium salt
- a complexant for the metal ion (often a carboxylic acid)
- surface-active chemicals
- mediator compounds

Recently, several overview papers have been published [e.g.80]. In the case of perpendicular magnetic media even very complicated compositions of, for instance, Co-Ni-Re-Mn-P have been discussed by Osaka [81]. The fundamental details of the electroless process in Co and Ni alloyed recording media are not well understood [82]. Some authors maintain that the mechanism is entirely electrochemical, thus controlled by electron transfer across the metal electrolyte interface, but others [82] prefer a process which is based on a surface-catalysed redox reaction without interfacial electron transfer.

Co-P layers have been produced for LMR for a long time. It was found for this particular film in [83] that the magnetic behaviour strongly correlates with the size and nature of the microcrystallites within the film.

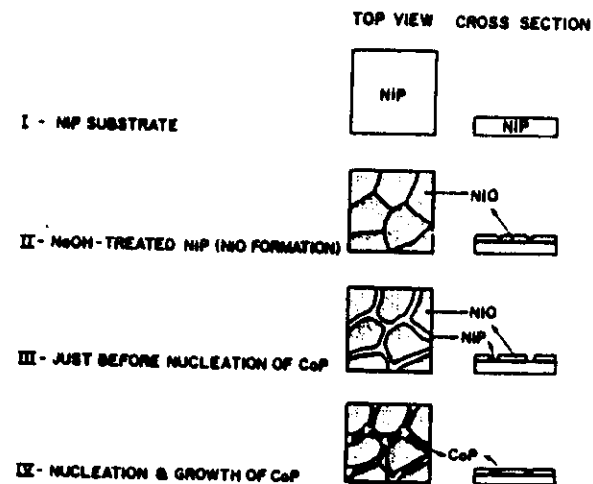


Figure 31. Model of the origin of the shape in electroless Co-P thin-film media.

Electrolytes that yield an average grain size close to the critical size for SDP have been found to result in high  $H_c$  deposits. Additionally it was found that a high  $S$  correlates with a small separation gap between the grains.

Another fact is that the type of substrate (in this case the underlayer) also influences the magnetic properties of the magnetic layer because it affects the nucleation and growth processes as well as the structure [e.g.84].

In fig.31 electroless Co-P was deposited on a Ni-P substrate that was pre-treated with NaOH. A good in-plane anisotropy was present. This type of treatment gives a Ni-oxide film of non-uniform distribution on the Ni-P substrate. Consequently on the NiO free surfaces the Co-P reaction starts growing in channels where the oxide is not available or is very thin. The shape of the magnetic crystals influences the shape anisotropy in the plane of the film.

Preparation and properties of the substrate play an important role. In general, the first step is to prepare the aluminium alloy basis by a deposition of a 6-50 micron thick Ni-P (non-magnetic) layer on top of it with a composition of 15-20 at% P, which is also non-magnetic.

The layer smoothes out all the defects of the base substrate. The hardness of the layer also improves the tribological effects. The next step is to polish and activate this layer and finally the magnetic layer (0.03-0.08 micron) is deposited. Mostly a wear-resistant layer (0.01 micron) is employed as a protective layer. Sometimes an antifriction layer is also applied.

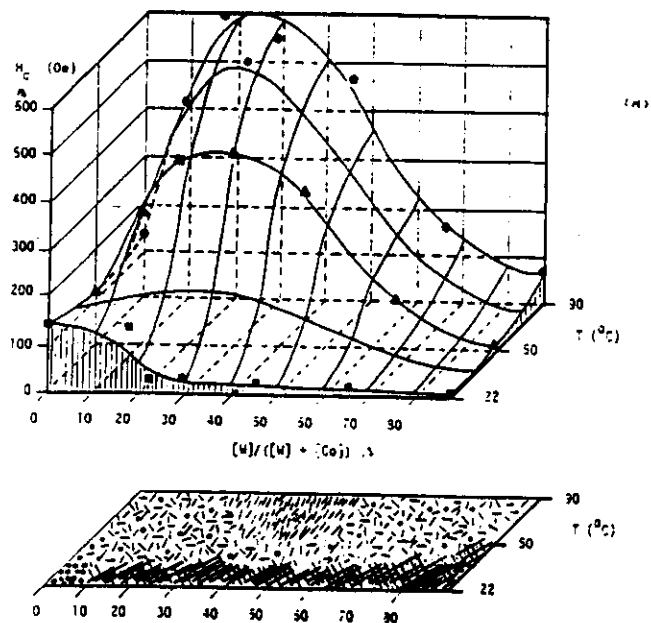


Figure 32. The in-plane coercivity as a function of bath composition and bath temperature. (Large-dots: fcc. Bars: hcp. Shaded areas: amorphous, small-dots: non-magnetic. The texture [0001] is illustrated by the degree of alignment of the bars.)

### 3.6. ELECTRODEPOSITION

Electrodeposition consists of two electrodes connected to an external current source. The metallic ions are reduced from an aqueous solution at the cathode.

Although electrodeposition is in principle more flexible than electroless deposition and much more complicated alloy compositions can be produced with this method, it has not been fully exploited and similar compositions are mainly found as those which are also used in electroless deposition. In the case of electrodeposition acidic solutions are often used.

A recent survey on electrodeposited Co-Ni-P layers is given in [85]. The structures of electrodeposited films are more complicated than those for electroless. The lower  $H_c$  materials form lamellar structures with an in-plane easy axis. The high  $H_c$  structures are more rod-like and shape anisotropy contributes to the coercivity. The platelets and rods are isolated by a thin non-ferromagnetic layer.

The growth of Co-Ni-P media is completely described by [86]. The magnetic properties vary with the thickness of the layer and are also dependent on the type of substrate such as Au, Cu or Ni-P. The grain size is large when Cu has been used.

A systematic investigation of the comparison between the bath composition, microstructure and magnetic properties for electrodeposited Co-W films is given in [87]. Co-W films are an outstanding example of a system in which a variety of metastable phase structures can be obtained by a proper choice of the deposition parameters. Both amorphous and crystalline structures were observed.

In fig.32 the in-plane  $H_c$  as a function of the basic bath composition for three different bath temperatures is given. In order to correlate the  $H_c$  to the microstructure the "phase diagram" is presented in the lower part of the figure. An explanation of the symbols used is: the large dots = fcc phase, bars = hcp, shaded area = amorphous, small dots = non-magnetic.

The [0001] texture is illustrated by the degree of alignment of the bars.

### 4. Summary And Conclusions

Particulate recording media have already been prepared with success for more than 25 years although they have certain disadvantages. For instance, only 40% of the coating volume consists of magnetic material in the case of tapes and floppies while only 20% in the case of hard disks.

The magnetisation in thin films is much higher than in particulate media because it is not diluted by a binder. In this case the material packing density is more or less 100%. However the "magnetic" packing density is lowered by voids, non ferromagnetic compositions, oxidation etc (see also the paper of Dr.Richter in this book). The properties can be easily changed by varying the deposition parameters. In the case of particulate media the whole chemical process has to be changed.

Thin films can contribute to the future needs in high density recording because they clearly show the possibilities for increasing linear and track densities. The presentations of the very high density recording systems have all used thin-film media.

Because for high density recording the film thickness (specially the longitudinal media) should be thin, an appropriate surface roughness is necessary therefore also very smooth substrate material is essential.

The corrosion behaviour of the thin (metal)-film media is still a difficult problem and material

improvement is needed as well as development of very thin overcoats as protection layers.

In the case of high density magnetic recording, the distance between the head and media should be extremely small. Therefore thin film media are good candidates [88].

Micromagnetic calculations, new magnetic analysing methods, advanced material sciences and development of new technologies have been the basic tools for obtaining the results of recent years. Although remarkable progress have been made there are still many problems to solve before a complete commercialised ultra-high density recording system will be available.

## 5 References

- [1]. T.Yogi, T.A.Hguyen, S.E.Lambert, G.L.Gorman and G.Castillo, IEEE Trans.on Magn. MAG-26, 1578 (1990) and the same issue page 2271.
- [2]. C.H.Bajorek, IBM Technical report, TR 07.903, (1988)
- [3]. Introduction to Magnetic Recording, ed. R.M.White, IEEE Press, New York, (1985);
- [4]. J.C.Mallison, The Foundations of Magnetic Recording, Academic press, Inc, London, (1987)
- [5]. C.D.Mee and E.D.Daniel, Magnetic Recording, Vol.I-III, McGraw Hill Publishing Company, (1987-1988); and the updated edition, Magnetic Recording Handbook, Technology & Applications (1990)
- [6]. A.S.Hoagland and J.E Monson, Digital Magnetic Recording, John Wiley & Sons, Inc. 2nd edition, (1990).
- [7]. K.Roll, J.Vac. Sci.Techn.A4(1), 14, (1986)
- [8]. G.Bate, in Ferromagnetic Materials, ed. by E.P.Wohlfarth, North Holland, Amsterdam, page 381. (1980)
- [9]. B.K.Middleton and C.D.Wright, IERE Conf.Proc.London No 54, 181, (1982).
- [10]. F.E.Luborsky, J.Appl.Phys. vol 32, 1918, (1961).
- [11]. R.D.Fischer and M.R.Khan, IEEE Trans.Magn.MAG-26(5), 1626, (1990).
- [12]. T.Wielinga, J.C.Lodder and J.Worst, IEEE Trans.Magn.,MAG-18, 1107, (1982)]
- [13]. T.Wielinga, Investigations on Perpendicular Recording, PhD-Thesis, University of Twente, Enschede, the Netherlands, (1983).
- [14]. S.Iwasaki and Y.Nakamura,IEEE Trans.Magn., MAG-13(5), 1272, (1977).
- [15]. E.Hirota, Chapter 12. in Physics and Engineering Applications of Magnetism, Y.Ishikawa and N.Miura (eds), Springer-Verlag,(1991)
- [15]. J.Simsova, J.C.Lodder, J. Kaczor, R.Gemperle, K.Jurek and I.Thomas, J.Magn. Magn. Mater., 73, 131, (1988).
- [16]. F.Schmidt and A.Hubert, J.Magn.Magn.Mater., 61, 307, (1986).
- [17]. J.N.Chapman, I.R.McFadden and S.McVitie,IEEE Trans. Magn. MAG-26, 1506, (1990)
- [18]. K.Yoshida, T.Okuwaki, N.Osakabe, H.Tanabe, Y.Horiuchi, T. Matsuda, K.Shinakawa, I.Tonumura and H.Fujiwara, IEEE Trans. Magn. MAG-19, 100, (1983)
- [19]. D.T.Pierce, J Ungaris and R.J.Celouta, MRS Bulletin 13, 19,(1988)
- [20]. D.Rugar, H.J.Mamin, P.Gruethner, S.E.Lambert, J.E.Stern, I.McFadden and T.Yogi, J.Appl.Phys.,68,1169, (1990)
- [21]. I.L.Sanders and S.E.Lambert, IEEE Proc. VLSI and Comp.Periph., 1-12, (1989).
- [22]. T.Yogi, T.A.Nguyen, S.E.Lambert, G.L.Gorman and G.Castillo, Mat. Res. Soc. Symp. Proc. Vol.232, 3-13, (1991).
- [23]. M.L.Williams and R.L.Comstock, AIP.Conf.Procs.5, 378,(1971)

- [24]. D.B.Richards and T.J.Szczecz, J.Appl.Phys.49(3), 1819, (1978)]
- [25]. E.Koster, H.Jakusch, U.Kullmann, IEEE Trans.Magn. 17(6), 2550, (1981)]
- [26]. T.Suzuki, IEEE Trans.Magn.20(5), 675, (1984)
- [27]. E.Samwel, P.R.Bissell and J.C.Lodder, Submitted to J. Appl. Phys. (1992).
- [28]. R.F. Burshah et al. eds., Deposition Technologies for Films and Coatings, Noyes publications, New Jersey (USA), (1982)
- [29]. D.S. Campbell, chapter 5 in Handbook of Thin Film Technology, McGraw-Hill, New York (1970), L.I. Maisel and R. Glang eds.
- [30]. K.L. Chopra, Thin Film Phenomena, McGraw-Hill, New York, (1969)
- [31]. R.Glang, chapter 1 in handbook of Thin Film Technology, McGraw Hill, New York (1970),eds. L.I.Maisel and R.Glang.
- [32]. L. Holland, Vacuum Deposition of Thin fFilms, Wiley, New York, (1956)
- [33]. Physical Vapour Deposition, ed. by R.J.Hill, Temascal, second edition, (1986).
- [34]. T. Wielinga et al. J. Phys E vol 13 (1980)]
- [35]. W.S. Hulscher, K.G. v.d. Berg and J.C. Lodder, Thin Solid Films, 9, 377-388, (1972)
- [36]. K.G. v.d. Berg, J.C. Lodder and T.C. Mensinga, Thin Solid Films, 34, 243-247, (1976)
- [37]. S.Takahashi, K.Umeda, E.Kita and A Tasaki, IEEE Trans Magn MAG-23(5), 3630, (1987)
- [38]. J.P.Lazzari, I Melnick and D Randet, IEEE Trans.on Magn. 3 (3) 205, (1967).
- [39]. D.E.Speliotos, G.Bate, J.K.Alstad and J.R.Morrison, J.Appl.Phys.,36, 972, (1965).
- [40]. D.O.Smith, M.S.Cohen and G.P.Weiss, J.Appl.Phys. vol 31, 1755, (1960).
- [41]. J.G.W van de Waterbeemd and G.W van Oosterhout, Philips Res. Reports 22, 375, (1967).
- [42]. A.G.Dirks and H.J.Leamy, Thin Solid Films, 47, 219, (1977); A.G.Dirks and H.J.Leamy, J.Appl.Phys, 49(6), 2430, (1978)]
- [43]. K.Hara, T.Hashimaoto and E.Tatsumaoto, J.Phys.Soc.Japan, 28,254,(1970); K.Hara J.Sci. Hiroshima.Ser.AII,34(2)139, (1970); K.Okamoto, T.hashimaoto, K.Hara. J.Phys. Soc. Japan 31 (5), 1374 (1971); K.Hara, T.Kamimori, and H.Fujiwara, Thin Solid Films,66, 185,(1980); T Hashimoto, K.Okamoto, K Hara, Thin Solid Films, 91, 145,(1982); H.Fujiwara, K.Hara, M.Kamiya, T.Hashimoto and K.Okamoto, Thin Solid Films vol.163,, 387, (1988);K.Okamoto, K.Hara, M.Kamiya, T.Hashimaoto and H.Fujiwara, Thin Solid Films.vol 176, 255,(1989); K.Okamoto, T.Hashimoto,H.Fujiwara, K.Hara and M.Kamiya, J.Magn.Magn.Mat, vol 81, 374 (1989)
- [44]. J.M.Nieuwenhuizen and H.B.Haanstra, Philips Techn.Rev., vol 27(1), 87,(1966)
- [45]. S.Keitoku, J.Sci.Hiroshima Iniv.,Ser A, vol 37, no2, 167, (1973)
- [46]. K.Nakamura, Y.Ohta, A.Ihto, IEEE Trans.Magn.MAG.18. no 6, 1077, (1982)
- [47]. T Kunieda, M.Odagiri, T.Fujita, EP 53 811 Al., 04.02.81, Bulletin 81/5, (1981).
- [48]. J.S.Gau et al J.Appl.Phys.61(8), 3807,(1987).
- [49]. G. Krijnen, S.B.Luitjens, R.W.de Bie and J.C.Lodder, IEEE Trans. Magn. MAG-.24(2), (1988).
- [50]. S.Swaving, G.J.Gerritsma, J.C.Lodder, Th.A.J.Popma, J.Magn.Magn.Mater.67, 155, (1987).
- [51]. T.C.Arnoldussen, E.M.Rossi, A Ting,A.Brunsch, J.Schneider and G.Tippel, IEEE Trans.on Magn. Mag-20,821,(1984).
- [52]. I.B.Puchalska, A.Hubert, S.Winkler and B.Mirecki,IEEE Trans.Mag. MAG-24(2), 1787, (1988); H.Aitlamine, M.Labrunne, I.B.Puchalska, IEEE Trans.Mag.MAG-26(1),48,(1990); H.Aitlamine, Propertes Magnetiques de Couches Minces de Ni-Co Elaborees sous Incidence Oblique, PhD Thesis, Universty de Paris 6, France, (1990); H.Aitlamine, L. Abelman and I.B.Puchalska, J.Appl.Phys. vol 71(1), 353, (1992).
- [53]. F.A.Pronk and J.C.lodder, IEEE Trans.Mag.MAG-24(2),1744, (1988); F.A.Pronk and

- J.C.Lodder, *J.de Physique*, Coll.C8, Suppl. No.12, Tome 49, 2005, (1988); H.v Kranenburg, J.C.Lodder, Y.Maeda, L.Toth and Th.J.A.Popma, *IEEE Trans.Mag.MAG-26*(5), 1620, (1990).  
 H.van Kranenburg, J.C.Lodder, Th.A.J.Popma, K.Takei and Y.maeda, *J.Magn.Soc.Jpn.*, vol 15, Suppl.No S2, 33, (1991);  
 [54]. G.K. Wehner, *Phys. Rev.* 108,35 (1957)  
 [55]. B. Chapman, *Glow Discharge Processes*, John Wiley & Sons, New York, (1980)  
 [56]. J.L. Vossen *J. Vac. Sci. Technol.* 8,512 (1971))  
 [57]. P. Sigmund, *Phys. Rev.* 184,383 (1974))  
 [58]. J.C. Cuomo and R.J. Cambino, *J. Vac. Sci. Technol.* 12, 79 (1975)  
 [59]. R.D. Bland et al., *J. Vac. Sci. Technol.* 11, 671 (1947)  
 [60]. A.G. Blachman, *J. Vac. Sci. Technol.* 10, 299 (1973)  
 [61]. J.J. Vossen and J.J. O'Neill, *RCA Review* 29, 566 (1986)  
 [62]. J.W. Patten and E.D. McClanahan, *J. Appl. Phys.* 43, 4811 (1972)  
 [63]. J.J. Vossen, *J. Vac. Sci. Technol.* 8, S12, (1971)  
 [64]. T Yogi, T.A.Nguyen, S.E.Lambert, G.L.Gorman and G.Castillo, *IEEE Trans.Magn.MAG-26*, 1578, (1990)  
 [65]. J.L. Vossen and J.J. Cuomo in *Thin Film Processes*, J.L. Vossen and W. Kern, Eds. Academic Press, New York, pp 11, (1978)  
 [66]. S.Nasu, K.Matsumoto, K Hashimimoto, K Saiki, *Jpn.J.Appl.Phys.*11 (2),61, (1987)  
 [67]. *Magnetic Materials: Microstructure and Properties*, MRS Vol. 232, eds. T Suzuki, Y.Sugita, B. Clemens, K.Ouchi and D.E.Laughlin, MRS Pittsburgh, Pennsylvania, (1991) [68]. C.A. Neugebauer, chapter 8 in *Handbook of Thin Film Technology*, McGraw-Hill, New York (1970), L.I. Maisel and R. Glang eds.  
 [69]. M. Volmer and A. Weber, *Z. Phys. Chem.* 119, 277 (1926)  
 [70]. F.S. Frank and J.H. v.d. Merwe *Proc. Roy. Soc., A* 198, 205 (1979)  
 [71]. I.N. Stranski and L. Krastanov *Sitzungsber. Akad. Wiss., Wien, Math. Naturwiss.* k1 II-b, 146, 797 (1938)  
 [72]. B.A. Movchan and A.V. Demchishin *Phys. Met. Metallogr.* 28, 83 (1969)  
 [73]. J.A. Thornton *Am. Rev. Mater. Sci.* 7, 239 (1977)  
 [74]. R. Messier et al. *J. Vac. Sci. Techn.* A2 (2), 500 (1984)  
 [75]. S.Muller-Pfeiffer, H van Kranenburg and J.C. Lodder, *Thin Solid Films*, (1992)  
 [76]. L.L. Chang and B.C. Giessen eds., *Synthetic Modulated Structures*, Academic Press, New York (1985)  
 [77]. See the various contributions in: *Materials for Magneto-Optic Data Storage*, edited by C.J.Robinson, T.Suzuki and C.M Falco, M.R.S. Proceedings 150, Pittsburg (1989).  
 [78]. P de Haan, Q Meng, T.Katayama and J.C.lodder, accepted for publication in *J.Magn.Magn.Mater.* (1992).  
 [79]. A.Brenner and G.E.Riddell, *J. Res Natl.Bur.Standards* 3, 31 (1946).  
 [80]. V.Bustic, J.Horkans and D.J.Barclay, page 250-283 in *Advances in Electrochemical Science and Engineering*, Vol.1, Eds H.Gerischer and C.W Tobias, (1990).  
 [81]. T.Osaka, Chapter 12, page 189-207, in *Perpendicular Magnetic Recording* eds. S.Iiwasaki and J Hokkyo, Ohmsha, IOS Press, Amsterdam, The Netherlands (1991).  
 [82]. P.Cavallotti and G.Salvago in *Proc. of Symposium on Electrodeposition Technology* Eds. L.T.Romankiw and D.R.Turner, The Electrochemical Society, Pennington, NJ (1987).  
 [83]. Tu Chen, D.A.Rogowski and R.H.White, *J.Appl.Phys.*49,1816 (1978).  
 [84]. M.Mirzamaani, L.Romankiw, C.McGrath, J.Mahlke and N.C.Andersen, *J.Electrochem. Soc.*135, 2813,(1988) and D.DiMilia, J.Horkans, C.McGrath, M.Mirzamaani and G.Scilla,

*J.Electrochem.Soc* 135,2817,(1988)

- [85]. D Pearce, D.Rice, and G.Tang, *Solid State Technology* 31 (11), 113 (1988).  
 [86]. A.Tago, T. Masuda and T. Taketa, *Rev.ECL of NTT (Tokyo)* 25, 1315 (1977).  
 [87]. U.Admon, M.P.Daniel, E.Grunbaum, J.C.Lodder, *J.Appl.Phys.*62 (5), 1943,(1987)  
 [88]. A.M.Hornola, C.M.Mate and G.B.Street, *MRS Bulletin*, vol XV,No.3, 45, (1990)